

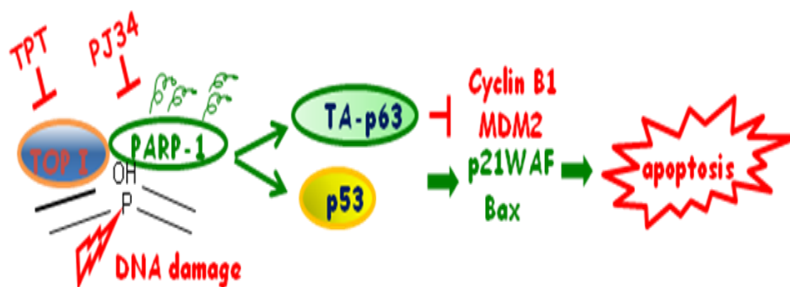


UNIVERSITA' DI NAPOLI FEDERICO II

DOTTORATO DI RICERCA IN BIOCHIMICA
E BIOLOGIA CELLULARE E MOLECOLARE
XXVI CICLO

Daniela Montariello

**Involvement of Poly(ADP-Ribose) polymerase inhibitors as
adjuvants of Topoisomerase 1 poisons
in the p53/p63-dependent threshold mechanism of the cell
fate decision between growth arrest and apoptosis.**



Academic Year 2012/2013



UNIVERSITA' DI NAPOLI FEDERICO II

**DOTTORATO DI RICERCA
BIOCHIMICA E BIOLOGIA CELLULARE E MOLECOLARE
XXVI CICLO**

**Involvement of Poly(ADP-Ribose) polymerase inhibitors as
adjuvants of Topoisomerase 1 poisons
in the p53/p63-dependent threshold mechanism of the cell fate
decision between growth arrest and apoptosis.**

**Candidate
Daniela Montariello**

Tutor
Prof. Piera Quesada

Coordinator
Prof. Paolo Arcari

Academic Year 2012/2013

Ringraziamenti

Al termine di questo percorso, desidero di ringraziare tutte le persone che hanno contribuito alla mia crescita sia professionale che umana.

Ho intrapreso questo cammino un po' inaspettatamente, avevo in mente altri progetti lavorativi, poi però sono stata entusiasta di cominciare un dottorato di ricerca nel gruppo della Prof. *Piera Quesada* che ha creduto in me sin da quando ero ancora una laureanda. E' chiaro che il più sentito ringraziamento va a lei, che mi ha sempre reputato all'altezza di ciò che stavo per intraprendere e mi ha seguito con un affetto "materno" da vicino e da lontano, anche durante l'esperienza all'estero, nella realizzazione degli esperimenti e... non solo.

Il primo incontro in laboratorio con la ricercatrice *Maria Malanga* ancora lo ricordo, ho capito subito che avrei avuto un valido riferimento scientifico per qualunque difficoltà.

Lei con la sua dolcezza, disponibilità e col suo rigore metodologico mi faceva pensare che tutto era possibile, senza mai scoraggiarmi. Purtroppo, quando prematuramente ci ha lasciato, la sensazione di aver perso un pilastro essenziale non solo nel lavoro, ma anche e soprattutto nella quotidianità ci ha accompagnato per diversi mesi e dopo un periodo buio, abbiamo finalmente ritrovato la luce, grazie anche alla solidarietà ricevuta dai colleghi del Dipartimento di Biologia.

Ringrazio caramente le ricercatrici *Daria Monti* e *Angela Arciello*, che si sono offerte di darmi una mano con le colture cellulari mettendo a disposizione i loro laboratori e la loro esperienza.

A settembre finalmente il gruppo di lavoro inizia a crescere ed arriva la prima tesista annuale... solo sulla carta, perchè di fatto *Mariella* è stata per me una compagna di avventure ed una valida spalla nella ricerca, oltre ad avermi presentato le sue due amiche storiche, *Conny* e *Melania*, con le quali ho trascorso uno dei periodi più belli all'università, tra pause caffè e confidenze sincere.

Poi è iniziata la collaborazione con le genetiste, dunque non posso fare a meno di ringraziare la Prof. *Viola Calabrò*, che ha illuminato molte scelte di lavoro offrendo il suo punto di vista da esperta biologa cellulare e la sua dottoranda *Annaelena Troiano*, per la sua cura e dedizione alle nostre cellule.

Un ringraziamento particolare va anche alla mia omonima *Daniela "2"*, che è subentrata nel nostro progetto come borsista e mi ha affiancato nel lavoro di ricerca nell'ultimo anno di dottorato.

Giornate lunghe, in attesa dei risultati, sono state rallegrate dalla presenza delle tesiste triennali *Imma*, *Marianna* e *Carmen*, che hanno reso meno pesanti periodi duri e stressanti e dall'ultima tesista annuale, *Laura*, che non

ho potuto accompagnare in seduta di laurea data la mia partenza per Zurigo, ma che ha concluso brillantemente il suo percorso anche senza di me.

Un altro “regalo” di *Maria Malanga* è stato per me l’opportunità di svolgere un periodo all’estero presso l’Università di Zurigo all’Istituto di Farmacologia e Tossicologia della Facoltà di Veterinaria, dove lei era molto apprezzata e stimata. Desidero ringraziare sinceramente il Prof. *Felix Althaus* che mi ha offerto questa possibilità e mi ha accolto per alcuni mesi nei suoi laboratori con la massima ospitalità e umanità.

In ultimo, ringrazio i miei riferimenti essenziali, quelli che ci sono ogni giorno e che mi hanno reso la persona che sono oggi. Senza di loro, non avrei mai raggiunto questo traguardo.

Summary

Poly(ADP-ribose) polymerase (PARP) inhibitors are thought as breakthrough for cancer treatment in solid tumours such as breast cancer through their effects on PARP's enzymatic activity. PARP enzymes are involved in the regulation of many cellular processes such as DNA repair, cell cycle progression and cell death.

Our previous findings showed that the hydrophilic PARP inhibitor PJ34 enhances the sensitivity of p53 proficient MCF7 breast carcinoma cells to topotecan, a DNA Topoisomerase 1 (TOP 1) inhibitor. It is already known that poly(ADP-ribosyl)ated PARP-1 and PARP-2 counteract TOP 1 poisons through non covalent but specific interaction of poly(ADP-ribose) (PAR) with some TOP 1 sites which results in inhibition of DNA cleavage and stimulation of the religation reaction. Moreover, repair of DNA strand breaks induced by poisoned TOP 1 is slower in the presence of PARP inhibitors, leading to increased toxicity.

In a first section, we combined the classical TOP 1 poison camptothecin or its water-soluble derivative topotecan with PJ34 to investigate the potentiation of chemotherapeutic efficiency in MCF7 (p53^{WT}), MDA-MB231 (p53^{mut}) breast carcinoma cells and SCC022 (p53^{null}) skin squamous carcinoma cells.

We showed that, following TPT/PJ34 combined treatment, MCF7 cells exhibit apoptotic death while MDA-MB231 and SCC022 cells are more resistant to these agents. Specifically, in MCF7, (i) PJ34 in combination with TPT causes a G2/M cell cycle arrest followed by massive apoptosis; (ii) PJ34 addition reverts TPT-dependent PARP-1 auto-modification and triggers caspase-dependent PARP-1 proteolysis; (iii) TPT, used as a single agent, stimulates p53 expression while in combination with PJ34 increases also the level of the pro-apoptotic isoform of p63 protein namely TAp63.

The identification of p63 proteins as new players involved in the cancer cell response to TPT/PJ34 is relevant for a better understanding of the PARP-1-dependent signaling of DNA damage. Furthermore, our data indicate that, in response to TPT-PJ34 combined chemotherapy, a functional cooperation between p53 and TAp63 proteins may occur and be essential to trigger apoptotic cell death.

A yet unsolved problem is the discrimination between covalent and non-covalent poly(ADP-ribosylation) (PARylation) of several nuclear proteins, including p53. Therefore, in a second section of the research, we got inside into this mechanism by using MCF7 breast carcinoma cells treated with topotecan, as we have demonstrated that they respond to DNA damage induced by topotecan treatment with p53 accumulation and PARP-1 auto-modification.

By using *in vitro* analyses we were able to identify the phosphorylated form of p53 at serine 15 residue as a target/acceptor of the PAR synthesized in the nuclei of damaged cells.

Furthermore, by cells co-immunoprecipitation experiments, it was found that PAR linked to PARP-1 interacts with p53 and is crucial for its nuclear stabilization.

In a third section we focused on the role/influence of PAR either in p53/p63 physical and functional interaction. For this part of the project, we compared again MCF7 and SCC022 cells with a different status of p53 as they showed a different sensitivity to apoptosis induced by TPT-dependent DNA damage.

Riassunto

Gli inibitori delle poli(ADP-ribosio) polimerasi (PARP) sono noti adiuvanti chemioterapici nel trattamento dei tumori solidi come il carcinoma mammario in base ai loro effetti sull'attività enzimatica delle PARP. Le PARP sono coinvolte nella regolazione di diversi processi cellulari quali il riparo del DNA, la progressione del ciclo cellulare e la morte cellulare.

Precedenti risultati hanno mostrato che l'inibitore di PARP idrofilico PJ34 incrementa la sensibilità delle cellule di carcinoma mammario MCF7 p53^{+/+} al topotecano, un inibitore della Topoisomerasi 1 (TOP 1). E' ormai noto che PARP-1 e PARP-2, in forma auto-modificata, contrastano l'effetto degli inibitori di TOP 1 mediante interazioni non covalenti ma specifiche del poli(ADP-ribosio) (PAR) con diversi siti di TOP 1, determinando l'inibizione del taglio al DNA e la stimolazione dell'attività di ricongiungimento ad opera di TOP 1. Pertanto, il riparo delle rotture sul DNA indotte dagli inibitori di TOP 1 è meno efficiente in presenza degli inibitori di PARP, che incrementano quindi la citotossicità dell'agente chemioterapico.

In una prima sezione, abbiamo combinato il classico veleno di TOP 1, la camptotecina, o il suo derivato idrosolubile topotecano al PJ34 al fine di valutare il potenziamento dell'efficienza chemioterapica in cellule di carcinoma mammario MCF7 (p53^{WT}) e MDA-MB231 (p53^{mut}) ed in cellule di carcinoma squamoso della cute SCC022 (p53^{null}).

E' stato osservato che, in seguito al trattamento combinato TPT-PJ34, le cellule MCF7 esibiscono morte apoptotica mentre le cellule MDA-MB231 e le SCC022 risultano più resistenti al trattamento con tali agenti. In particolare, in MCF7, (i) il PJ34 in combinazione con TPT causa un arresto del ciclo cellulare in fase G2/M, seguito da massiva apoptosi; (ii) l'aggiunta di PJ34 reverte l'auto-modificazione di PARP-1 dipendente da TPT e determina la proteolisi di PARP-1 caspasi-dipendente; (iii) il TPT, usato come agente singolo, stimola l'espressione di p53, mentre in combinazione col PJ34 incrementa i livelli di espressione della isoforma pro-apoptotica della proteina p63 denominata TAp63.

L'identificazione delle proteine p63 come nuovi effettori coinvolti nella risposta delle cellule tumorali al trattamento TPT-PJ34 è di rilevante importanza per la comprensione della segnalazione del danno al DNA ad opera di PARP-1. I nostri risultati indicano che, in risposta ad una chemioterapia combinata TPT-PJ34, un'interazione funzionale tra le proteine p53 e TAp63 potrebbe avvenire ed essere essenziale all'innesco del processo apoptotico.

Un problema ancora irrisolto è quello di discriminare tra poli(ADP-ribosilazione) (PARilazione) covalente e non covalente di diverse proteine nucleari, tra cui p53. Pertanto, in una seconda sezione della ricerca, tale

meccanismo è stato definito utilizzando cellule di carcinoma mammario MCF7 trattate con topotecano, avendo dimostrato che esse rispondono al danno al DNA ad opera del TPT con accumulo di p53 ed auto-modificazione di PARP-1.

Mediante saggi *in vitro* la forma fosforilata di p53 in serina 15 è stata identificata quale bersaglio/accettore del PAR sintetizzato nei nuclei delle cellule danneggiate.

Inoltre, mediante co-immunoprecipitazione in cellule si è osservato che il PAR legato a PARP-1 interagisce con p53 ed è cruciale per la sua stabilizzazione nucleare.

In una terza sezione, abbiamo infine valutato se il PAR è in grado di influenzare l'interazione fisica e funzionale tra p53 e p63. In questa parte del progetto, abbiamo nuovamente paragonato le cellule MCF7 ed SCC022 a diverso stato di p53, in quanto esse hanno mostrato una diversa sensibilità all'apoptosi indotta da un danno al DNA TPT-dipendente.

Index

	Pag.
1. Introduction	1
1.1 The role of Poly(ADP-ribose) polymerase (PARP) in the DNA damage signaling network	
1.2 Evolution of PARP inhibitors: from concept to the clinic	5
1.3 DNA Topoisomerase 1 (TOP 1) inhibitors as chemotherapeutic agents	6
1.4 The p53/p63 superfamily	8
1.5 Scientific hypothesis and aim of the work	10
2. Materials and Methods	11
2.1 Drugs, media, antibodies and chemicals	
2.2 Cell cultures and transfection	11
2.3 Cell treatments	12
2.4 Cytofluorimetric analysis	12
2.5 Isolation of nuclear and post-nuclear fractions	12
2.6 Western blot analyses	13
2.7 PARylation in nuclear fraction and on recombinant proteins	13
2.8 PAR electrophoretic mobility shift assay	14
2.9 Co-Immunoprecipitation	15
3. Results Section 1: p63 involvement	16
3.1 Effect of PJ34 on CPT/TPT-induced growth inhibition and cell cycle distribution in human carcinoma cells	
3.2 Analysis of CPT- or TPT-dependent TOP 1 inactivation	19
3.3 Analysis of PAR synthesis in carcinoma cells after treatment with TPT ± PJ34	20
3.4 Involvement of p63 in the cell response to TPT ± PJ34 treatment	22
Results Section 2: p53 PARylation	24
3.5 PARylation in isolated nuclei	
3.6 <i>In vitro</i> p53 PARylation	26
3.7 p53 PARylation in TPT treated MCF7 cells	28
Results Section 3: Involvement of PARP inhibitors in the p53/p63 signaling pathway	29
4. Discussion	32
5. References	36

List of Tables and Figures

	Pag.
Figure 1. The poly(ADP-ribosyl)ation reaction	2
Figure 2. Structural and functional characteristics of PARP-1	3
Figure 3. Role of PARP-1 in DNA repair	4
Figure 4. Topoisomerase 1 catalytic cycle	7
Figure 5. Gene architecture of p53 family	9
Figure 6. Dose-dependent response of MCF7 cells treated with CPT/TPT and PJ34 as single agents or in combination	16
Figure 7. Cell growth inhibition in MCF7, MDA-MB231 and SCC022 cells treated with CPT and PJ34 as single agents or in combination	17
Figure 8. Cell cycle analysis of MCF7 cells subjected to TPT and PJ34 single and combined treatments	18
Figure 9. Western blot analysis of TOP 1 soluble fraction in carcinoma cells untreated or 48 h treated with the indicated drugs	19
Figure 10. Analysis of TPT-dependent PARP-1 activation or PJ34-dependent PARP-1 inhibition in carcinoma cells untreated or 48 h treated with the indicated drugs	21
Figure 11. Western blot analysis of p53, p63, p21WAF, MDM2 and cyclin B1 expression in MCF7 cells untreated or 48 h treated with the indicated drugs	22
Figure 12. Western blot analysis of protein extract from nuclear and cytoplasmic fraction of MCF7 cells untreated or 48 h treated with the indicated drugs	23
Figure 13. Western blot analyses of nuclei isolated from MCF7 cells untreated or 1 h treated with TPT 10 μ M	24
Figure 14. <i>In vitro</i> PARylation assays	26
Figure 15. PAR EMSA	27
Figure 16. Western blot analyses of co-immunoprecipitation of MCF7 cells 48 h treated with TPT 2.5 μ M	28
Figure 17. Western blot analysis of protein extract from SCC022 cells untreated or treated with TPT \pm PJ34 before and after p53 transfection	30
Figure 18. Western blot analysis of protein extract from SCC022 cells transfected for p53 and/or TAp63 γ and treated with TPT + PJ34	31

1. Introduction

1.1 The role of Poly(ADP-ribose) polymerase (PARP) in the DNA damage signaling network

The structural integrity of the chromosomes is maintained by checkpoint pathways protecting cells and organisms from functional disturbances in DNA and cell cycling.

In higher eukaryotes, DNA strand breaks, either generated directly by ionizing radiation and oxidizing agents or arising as intermediates of repair processes, are sensed by an abundant, 113-kDa nuclear enzyme, Poly(ADP-ribose) polymerase-1 (PARP-1). This is a member of a large family of enzymes with a homologous catalytic domain but with otherwise distinct structures, functions and localizations. PARP-1 binds with high affinity to DNA strand interruptions via 2 N-terminal zinc finger modules, with consequent activation of its catalytic C-terminal domain. Activated PARP-1 uses β -NAD⁺ as a substrate to catalyze its auto-modification as a homodimer and, to a lesser extent, the modification of other nuclear proteins, with ADP-ribose chains (**Figure 1**). Through recruitment of specific proteins at the site of damage and regulation of their activities, these polymers may either directly participate in the repair process or coordinate repair through chromatin unfolding, cell cycle progression and cell survival/cell death pathways.

Another nuclear member of the PARP family, PARP-2, is also able to catalyze DNA damage-dependent auto-modification and can homo- or hetero-dimerize with PARP-1. Although PARP-2 accounts for only 10%–15% of the cellular poly(ADP-ribosylation) (PARylation) capacity under conditions of genotoxic stress, it can partially compensate for PARP-1 loss in knockout mice. Simultaneous deletion of both *parp-1* and *parp-2* genes is incompatible with development; embryos die at the onset of gastrulation.

In DNA-damaged cells, increased poly(ADP-ribose) (PAR) synthesis due to PARP-1 and PARP-2 activation is paralleled by an accelerated catabolism that reduces polymer half life from several hours to a few seconds. This allows rapid reversal of PARPs' auto-modification and ensures that elevated PAR levels are present only transiently in the cell. An evolutionarily conserved enzyme, poly(ADP-ribose) glycohydrolase (PARG) is responsible for the specific degradation of polymers to monomeric ADP-ribose units (*Malanga et al; 2005*). It can be postulated that PARG endoglycosidic activity generates free PAR from PARylated protein, that could still interact with basic proteins, for example with constitutive components of chromatin, enzymes and transcription factors. Furthermore, an alternative PAR-degradation pathway has been described resulting from the action of ADP

Introduction

of PARP-1, the product PAR displays a tree-like structure, forming a highly negative charged cloud at the covalently modified protein, which impacts on functionality probably through electrostatic repulsion of affected enzymes from DNA.

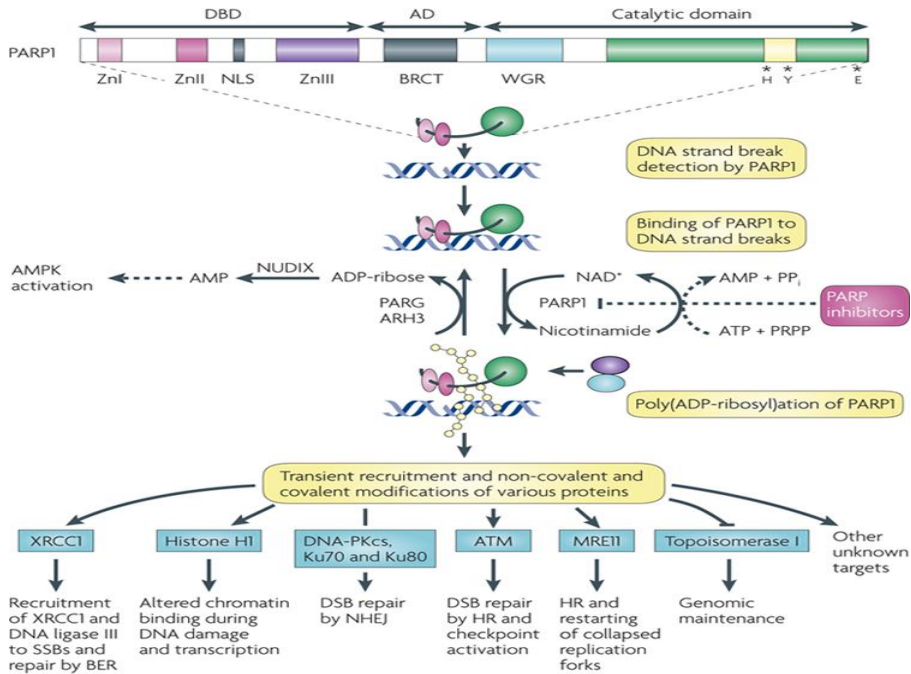


Figure 2. Structural and functional characteristics of PARP-1.

The main acceptor of PAR is PARP-1 itself, but also its interaction partners can be modified, as shown for several nuclear proteins *in vitro* and *in vivo*. In addition to covalent modification, proteins can interact with PAR in a non-covalent fashion. So far, three different motifs have been described: first, a sequence of basic and hydrophobic residues, the so called PAR-Binding-Motif (PBM), which is present in many proteins involved in maintaining genomic stability, i.e., telomerase, p53, histones, base-excision-repair (BER) platform protein XRCC1, nucleotide-excision-repair (NER) protein XPA and many more. Next, it was reported that the macro-domain binds in an end-capping mode to the tip of a PAR chain. Both principles, covalent and non-covalent interaction, can be present side-by-side within one protein. For example, the tumour suppressor p53 displays three covalent as well as three non-covalent binding sites. Interestingly, the interaction partner is one determinant that affects complexity of PAR, i.e., chain-length and branching.

Additionally, proteins differ in their ability to bind to different PAR structures. In summary, PARP-1 (respectively its product PAR) is able to change the surrounding environment by either excluding modified proteins from distinct sites, or by attracting factors containing PAR interaction-motifs (*Beneke; 2012*).

At the same time, the formation of PAR reduces the affinity of PARP-1 and histones for DNA, providing a mechanism for removing PARP-1 from damaged sites and for the local modulation of chromatin compaction. The removal of PARP-1 provides access for repair proteins, but the enzyme remains in the vicinity of the breaks, recruiting other selected proteins into multiprotein complexes to accelerate DNA damage repair (*Rouleau et al; 2010*). In contrast, when DNA damage exceeds cell repair capacity, PARP-1 undergoes cleavage by caspases (3 and 7) into two fragments of 89 kDa and of 24 kDa, thereby avoiding futile cycling of PAR that would otherwise deplete the cell of β -NAD⁺ required for the onset of apoptosis (*Scovassi et al; 1999*).

PARP-1 and PARP-2 play a dual role as damage sensors and signal transducers to down-stream effectors (**Figure 3**).

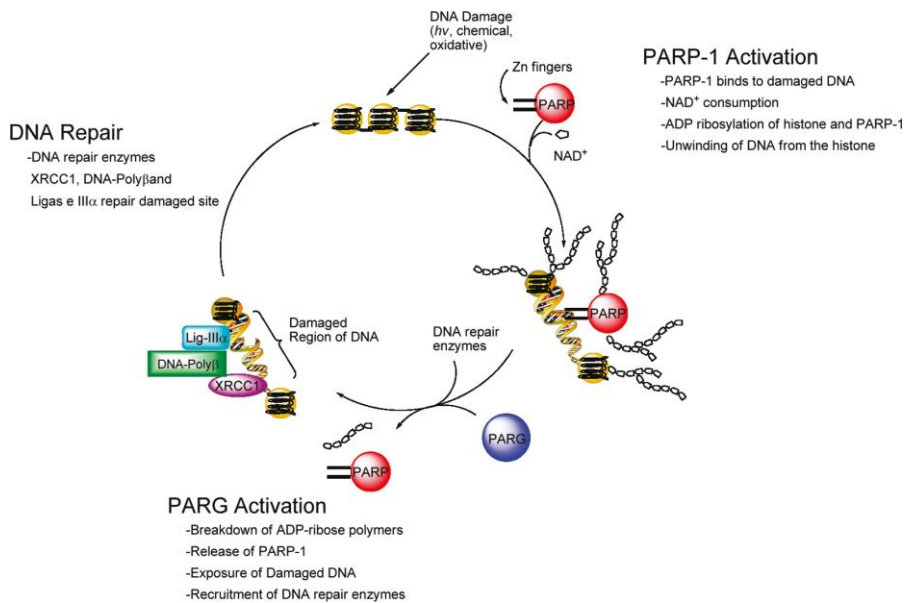


Figure 3. Role of PARP-1 in DNA repair.

Both proteins share several common nuclear binding partners and have been described as contributors to base excision repair (BER).

In fact, PARP-1 interacts with X-ray repair cross-complementing 1 (XRCC1), DNA polymerase β and DNA ligase III, which are involved in BER (Schreiber *et al*; 2002).

PARP-1 is also involved in DSBs repair process. Eukaryotes have two pathways for repairing DSBs: homologous recombination (HR) and non homologous end joining (NHEJ). The relative contribution of these two DSBs repair pathways seems to differ depending on the cell cycle phase: HR acts mainly in the S and G2 phases and NHEJ mostly in the G1 phase (Khanna *et al*; 2001).

In regard HR, PARP-1 interacts with both ATR and ATM kinases suggesting another susceptible pathway for PARP inhibitors induced apoptosis (Haince *et al*; 2007). Cell cycle checkpoint activation and growth arrest in response to DNA damage rely on the ATM/ATR kinases and their downstream targets like p53 (Yoon *et al*; 2012). p53 activates p21WAF which binds PARP-1 during base excision repair (Cazzalini *et al*; 2010). Indeed, PARP-1 is reported to interact with and poly(ADP-ribosyl)ate the DNA-PK subunit Ku, an important factor of the alternative pathway NHEJ (Wang *et al*; 2006).

1.2 Evolution of PARP inhibitors: from concept to the clinic

The inhibition of PARP has two potential therapeutic applications for drug discovery. The first application is as a chemopotentiator, since many anticancer therapeutics target DNA damage as a mechanism to destroy rapidly dividing cancer cells. Thus, the PARP mediated repair pathway is one major mechanism for DNA repair by many cancerous cell types leading to drug resistance and continued tumour growth. Hence, PARP inhibition in combination with DNA damaging chemotherapeutics or radiation would compromise the cancer cell DNA repair mechanisms, resulting in genomic dysfunction and cell death.

The second, a more recent discovery, is that PARP can be used as a stand-alone therapy for tumour types that are already deficient in certain types of DNA repair mechanisms. Breast cancer associated genes BRCA1 and BRCA2 have long been characterized as tumour suppressor genes that play an integral role in the repair of DSBs in DNA through HR process. The increase of DSBs in the presence of HR deficient cell types leads to chromosomal aberrations and instability of the genome resulting in cell death (synthetic lethality). This research supported the hypothesis that PARP inhibitors could be used as single agents in cancer cell types with deficient DNA repair mechanisms (Ferraris; 2010).

The potential of PARP inhibitors to increase the efficacy of chemotherapy has led to the development of a wide range of specific inhibitors-quinazolinone derivatives– like NU1025 and PJ34, which display increased potency compared to the prototype 3-aminobenzamide (3-ABA) (*Sandhu et al; 2010*).

Certain PARP inhibitors including PJ34 induce a G2/M arrest when used in conjunction with methylating agents (*Tentori et al; 2005*) cisplatin (*Sandhu et al; 2010*) and Topoisomerase 1 poisons such as camptothecin (CPT) or its watersoluble derivative topotecan (TPT) (*Smith et al; 2005*), highlighting the existence of potentially different outcomes from PARP inhibition whose molecular mechanisms have not yet been conclusively determined.

1.3 DNA Topoisomerase 1 (TOP 1) inhibitors as chemotherapeutic agents

The compact and supercoiled nature of the DNA double helix requires topological modification during important cellular processes such as transcription, replication and repair. This modification is conducted by DNA Topoisomerases and involves transient cleavage and religation of the double-stranded DNA molecule. Topoisomerases are enzymes that cleave one or both of the sugar-phosphate backbones of double-stranded DNA, without altering its chemical composition (hence the term ‘isomerase’). Type 1 Topoisomerases (TOP 1) cut a single strand of DNA to allow relaxation of torsional stresses before re-annealing. This mode of catalysis involves an intermediate known as the *cleavage complex*, which comprises the Topoisomerase enzyme attached to the cleaved DNA by a covalent phosphotyrosyl bond (*Gilbert et al; 2012*).

Camptothecin (CPT), the prototype of TOP 1 inhibitors, and its derivatives such as the clinically relevant drug topotecan stabilize the *cleavage complex* in the *abortive complex*, and thus prevents religation step of the enzyme catalytic cycle, generating an accumulation of SSBs (**Figure 4**). The cytotoxic mechanism of camptothecins is largely S-phase-dependent, indicating that is triggered by a collision between replication fork and the *abortive complex*. This may result in blockage of fork movement, and finally, the formation of DNA DSBs (*Tomicic et al; 2005*).

The camptothecin derivative Topotecan (TPT) is approved for the treatment of ovarian cancer, non small-cell lung cancer and under clinical investigation for a number of advanced solid tumours and haematological malignancies (*Pommier et al; 2006*).

For the reason that HR is S-phase-dependent, TOP 1 poisons-induced replication-dependent DSBs are usually repaired by the HR pathway.

It is known that PARP inhibitors increase the cytotoxic effects of TPT. Furthermore, the molecular mechanism underlying tumour chemosensitization to TOP 1 poisons by PARP inhibitors has been in part clarified by recent findings showing that PARP-1 and -2, in their auto-modified form, counteract camptothecin action facilitating resealing of DNA strand breaks. This occurs through non covalent yet specific interaction of PAR with particular TOP 1 sites which results in inhibition of DNA cleavage and stimulation of the religation reaction (*Malanga et al; 2004*).

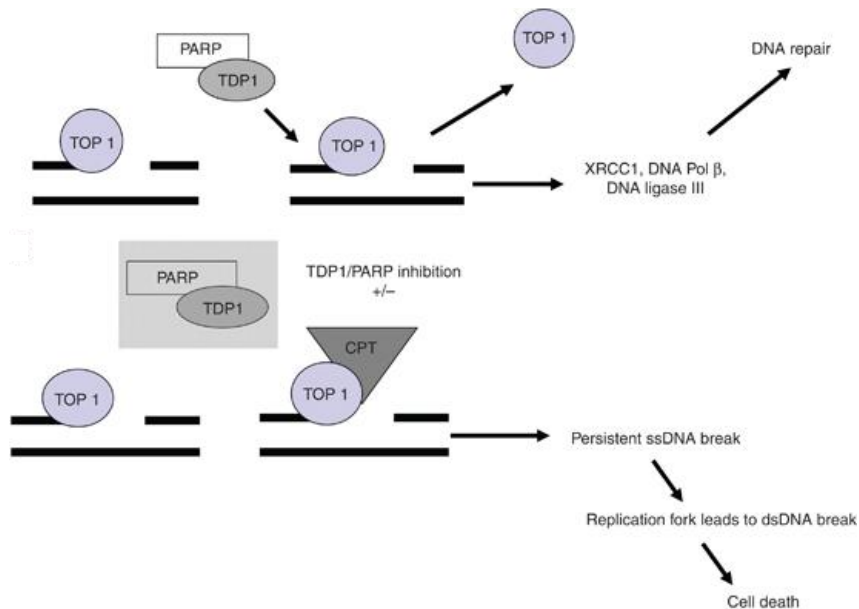


Figure 4. Topoisomerase 1 catalytic cycle.

In this regard, it has been previously demonstrated that PJ34 can positively or negatively modulate p53 and its target p21WAF depending of the cell genetic background (*Cimmino et al; 2007*) or DNA damage stimulus, i.e., cisplatin (*Gambi et al; 2008*) or TPT (*D'Onofrio et al; 2011*). Indeed, regulating p21WAF expression is one model whereby PARP inhibitors, following the activation of different checkpoint pathways, can cause cell cycle arrest. It has recently been reported that in breast carcinoma MCF7 cells, PJ34 causes a p21WAF-dependent mitotic arrest and that neither PARP-1 nor p53 is required for this mechanism (*Madison et al; 2011*). Furthermore, in triple negative breast cancer cell lines, PJ34 synergizes with cisplatin by reducing the levels of $\Delta Np63\alpha$ with a concurrent increase of p21WAF (*Hastak et al; 2010*).

On the light of all these evidences, the use of chemical inhibitors of PARP in combination with TOP 1 inhibitors CPT or TPT appears to be a promising approach to enhance the antitumour activity of these compounds.

1.4 The p53/p63 superfamily

A factor supposed to be involved in determining the sensitivity of cells to TOP 1 inhibitor is p53. p53 plays a key role in transduction pathways induced by several types of cellular stress by regulating the expression of gene products that can either lead to cell cycle arrest, thereby preventing the replication of DNA before the damage is repaired, or cause cell death by apoptosis (*Lane et al; 2003*). p53 is a target of a plethora of post-translational modifications (i.e. phosphorylation, acetylation, ubiquitination, methylation) and these most likely regulate or integrate its sub-cellular distribution, function and interaction partners (*Dai et al; 2010*). Moreover, it has been reported that PARP-1 is a positive regulator of p53 (*Wieler et al; 2003*) and that PARP inhibition enhances p53-dependent and p53-independent DNA damage responses induced by DNA damaging agents (*Nguyen et al; 2011*).

Several nuclear proteins including p53 are PARylated by non-covalent interaction with PAR chain linked to PARP-1 (*Malanga et al; 2005*). Previous results have shown that p53 protein is able to strongly interact with PAR by means of 3 polymer binding motifs (PBMs) (*Gagnè et al; 2008*). However, it has been reported that in response to DNA damage, a covalent p53 PARylation is able to promote accumulation of p53 in the nucleus, where it exerts its transactivation function (*Kanai et al; 2007*). On the other hand, it has been quantified PAR binding affinity (10^{-7} - 10^{-9} M range) of several proteins (i.e. p53, XPA, DEK) as a function of chain length (*Fahrer et al; 2010*). They have shown that among them only p53 is able to interact with both short and long PAR chains with equivalent affinity.

Δ Np63 α is a member of the p53 protein family highly expressed in squamous cell carcinoma and invasive ductal breast carcinoma (*Di Costanzo et al; 2012*). Δ Np63 α and p53 have been shown to inversely regulate target genes such as p21WAF in the context of DNA damage (*Schavolt et al; 2007*). Owing to the presence of two promoters, the p63 gene encodes two major classes of proteins: those containing a transactivating (TA) domain homologous to the one present in p53 (i.e. TAp63) and those lacking it (i.e. Δ Np63) (*Di Costanzo et al; 2011*). In addition, alternate splicing at the carboxy-terminal (C-terminal) generates at least three p63 variants (α , β and γ) in each class (**Figure 5**). The TAp63 γ isoform resembles most p53, whereas the α isoforms include a conserved protein-protein interaction domain named Sterile Alpha Motif (SAM). TAp63 proteins mimic p53

Introduction

function including transactivating many p53 target genes and inducing apoptosis, whereas the $\Delta Np63\alpha$ protein, has been shown to repress p53-target genes acting as an oncogene (Yang *et al.*; 1998).

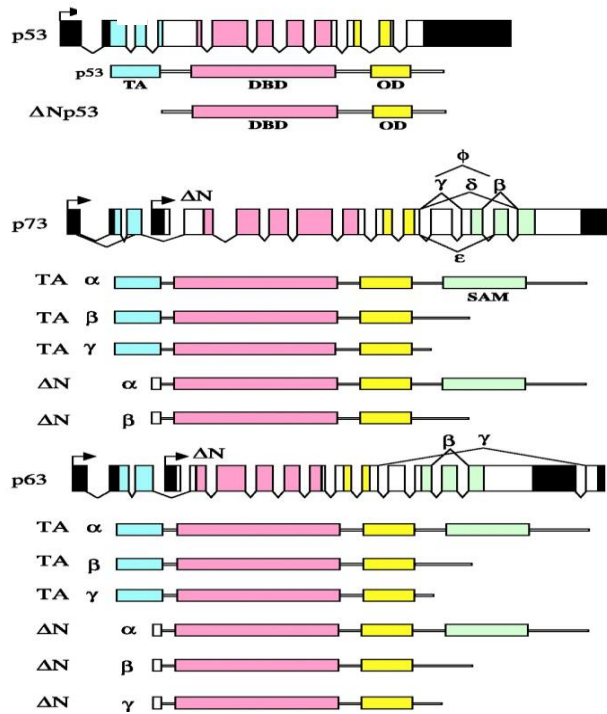


Figure 5. Gene architecture of p53 family.

Their structural similarities allow for both physical and functional interactions among the three p53 family members. The highest degree of homology among them is observed within the DBD (>60% amino-acid identity between p53 and both p63 and p73, and ~ 85% amino-acid identity between p63 and p73), including conservation of all essential DNA contact residues (De Laurenzi *et al.*; 2000).

This finding implied that all three genes might regulate a shared subset or transcriptional target genes. Secondly, p53 protein(s) are required to form tetrameric complexes in order to function as a transactivator, and the oligomerization domain shared by all the three family members is highly homologous. The formation of hetero-tetramers composed of multiple p53 family members might therefore represent another means of functional interaction.

Indeed, cotransfection studies showed that p63 and p73 co-associate when ectopically overexpressed, while p53 binds more weakly to either p63 and p73 (*Chan et al; 2004*). Interestingly, residues implicated in the PAR binding domains identified in the p53 DBD (*Malanga et al; 1998*) are also conserved in p63 and p73.

1.5 Scientific hypothesis and aim of the work

From the mean of such evidences, we have investigated the effect of PJ34 used as a single agent or in association with CPT or TPT in the DNA damage response of mammary breast cancer cells (MCF7^{p53^{wt}} and MDA-MB231^{p53^{mut}}) and skin squamous carcinoma cells (SCC022^{p53^{null}}) showing an active involvement of p53 and p63 in the cellular response to these agents.

We postulate that the sensitivity to combined treatments is mediated by sustained DNA damage/inefficient DNA repair triggering p53 and TAp63-mediated apoptosis.

In a second section of our study, we have used different experimental approaches to analyze p53 PARylation either in living cells, in nuclei and *in vitro* with the aim to discriminate between its covalent and/or non-covalent modification. As a model system, we used MCF7 cells subjected to TPT ± PJ34 treatments to perform PARP-1 and p53 co-immunoprecipitation experiments. In isolated nuclei, we immunodetected the PAR induced by TPT-dependent DNA damage and its target protein(s). Furthermore, for *in vitro* enzymatic assays we used human recombinant PARP-1 enzymes and p53 protein while for PAR-EMSA purified PAR.

In a third section, we focused on the role/influence of PAR either in p53/p63 physical and functional interaction. For this part of the project, we compared again MCF7 and SCC022 cells with a different status of p53 as they showed a different sensitivity to apoptosis induced by TPT-dependent DNA damage. That for we need to transfect cells and work with ectopically expressed p53 and/or p63 for immunological analyses.

2. Materials and Methods

2.1 Drugs, media, antibodies and chemicals

CPT and TPT were from *Glaxo Smith-Kline*, PJ34 [N-(6-oxo-5,6-dihydrophenanthridin-2-yl)-(N,N-dimethylamino) Acetamide] was from *Alexis Biochemicals*. The cocktail of protease inhibitors was from *ROCHE-Diagnostic*.

MCF7, MDA-MB231 and SCC022 cells were from *CLS Cell Lines Service*, Dulbecco's modified Eagle's medium (DMEM), heat-inactivated foetal bovine serum (FBS), Roswell Park Memorial Institute (RPMI) medium and Lipofectamine 2000 were from *Invitrogen*; penicillin, streptomycin and L-glutamine were from *LONZA*.

6-biotin-17-NAD (Bio-NAD) and anti-PAR mouse monoclonal antibody (4335) were supplied by *TREVIGEN*.

PVDF (poly-vinylidene-fluoride) and nitrocellulose membranes were from *MILLIPORE S.p.A*. Not-fat-milk power was from *EUROCLONE*.

Anti-DNA TOP 1 (Sc1-70) human antibody was from *Topogen*. Recombinant p53 (RRM2B), anti-PARP-1 (C2-10), anti-p63 (4A4), anti-p53 (DO-1), anti-p21WAF (F-5), anti-cyclin B1 (V152), anti-AIF (E-1), anti-GAPDH (6C5) mouse monoclonal antibodies and anti-p53 (FL-393), anti-actin (H-196) rabbit polyclonal antibodies and protein A/G PLUS Agarose were from *Santa-Cruz Biotechnology*. Anti-phospho-p53(ser15) (9284), anti-PARP-1 (9542), anti- γ H2AX (ser139, 2577), anti-Bax (D2E11) rabbit polyclonal antibodies and anti-biotin (D5A7) rabbit monoclonal antibody were from *Cell Signaling*. Anti-MDM2 (Ab-2) mouse monoclonal antibody was from *Oncogene Research Products*. Anti-PAR (10H) mouse monoclonal antibody, PARP-1 human recombinant wild-type and [$E^{988}K$] mutated were from *Alexis Biochemicals*. Goat anti-mouse and goat anti-rabbit IgG HRP-conjugated antibodies were from *Sigma-Aldrich*.

All other chemicals analytical grade were of the highest quality commercially available.

2.2 Cell cultures and transfection

Breast cancer-derived MCF7^{p53wt} and MDA-MB231^{p53mut} cells were maintained in Dulbecco's modified Eagle's medium (DMEM) containing 10% (v/v) heat-inactivated foetal bovine serum (FBS), while squamous SCC022^{p53 null} carcinoma cells were maintained in Roswell Park Memorial Institute (RPMI) medium containing 10% (v/v) FBS, 100 U/ml penicillin, 100 g/ml streptomycin, 5 mM L-glutamine and incubated at 37 °C in a

humidified atmosphere, plus 5% CO₂. Cell transfection was performed using Lipofectamine 2000 (*Invitrogen*) following the manufacturers' protocols.

2.3 Cell treatments

Cells were seeded at 1×10^6 cells in 10 ml and 24 h after seeding, treated with 1 μ M CPT (stock solution 1 mM DMSO) or 5 μ M TPT, 10x IC50 (*Devy et al; 2004*), 10 μ M or 20 μ M PJ34 alone and in combination for 48 h in fresh medium. Culture medium was removed and, after PBS wash, cells were recovered 6×10^6 cells/ml in 50 mM Tris-HCl pH 7.5, 150 mM NaCl, 5 mM EDTA, 1% NP40 (Lysis Buffer) plus 2 mM PMSF and 1:25 dilution of protease inhibitors cocktail solution. After 40 min of incubation on ice, cellular suspensions were scraped and centrifuged at 16,000 x g for 20 min at 4 °C.

Cell growth inhibition was assessed by cell counting at different time points (0–24–48h) or by the 3-[4,5-dimethylthiazol-2-yl]-2,5-diphenyltetrazolium bromide (MTT) assay using 1×10^4 48 h treated cells. The experiments were performed in triplicate.

2.4 Cytofluorimetric analysis

Control and treated cells were fixed in 70% ethanol and stored at -20 °C until analysis. After a washing in PBS w/o Ca²⁺/Mg²⁺, cells were stained in 2 ml of propidium iodide (PI) staining solution [50 μ g/ml of PI, 1 mg/ml of RNase A in PBS w/o Ca²⁺/Mg²⁺, pH 7.4] overnight at 4 °C and DNA flow cytometry was performed in duplicate by a FACScan flow cytometer (*Becton Dickinson Franklin Lakes*) coupled with a CICERO work station (*Cytomation*). Cell cycle analysis was performed by the ModFit LT software (*Verity Software House Inc. Topsham*). FL2 area versus FL2 width gating was done to exclude doublets from the G2/M region. For each sample 15,000 events were stored in list mode file.

2.5 Isolation of nuclear and post-nuclear fractions

To isolate sub-cellular fractions, 3×10^6 cells were suspended in 200 μ l of 30 mM Tris-HCl pH 7.5 buffer, containing, 1.5 mM MgCl₂, 10 mM KCl, 1% (v/v) Triton X-100, 20% glycerol, 2 mM PMSF and 1:25 dilution of protease inhibitors cocktail solution. After 30 min of incubation on ice, cellular suspensions were centrifuged at 960 x g for 90 sec at 4 °C and the

nuclear fractions recovered in the pellet. The supernatant represents the cytoplasmic fraction.

Nuclear fractions were resuspended in 50 μ l of 20 mM HEPES pH 7.9 buffer, containing 20 mM KCl, 0.2 mM EDTA, 1.5 mM MgCl₂, 25% glycerol and the protease inhibitors cocktail solution. Protein concentration was determined using the Bradford protein assay reagent (*BIO-RAD*), with bovine serum albumin as a standard.

2.6 Western blot analyses

Aliquots of 10 μ l of cellular proteins (approx 50–100 μ g) were separated by 10% SDS-PAGE and transferred onto a PVDF membrane using an electroblotting apparatus (*BIO-RAD*). The membrane was subjected to immunodetection after blocking with 5% non-fat milk in TBST 1 h, with anti-PARP-1 (C2-10; diluted 1:2,500), anti-TOP 1 (Scl-70; diluted 1:1,000), anti-PAR (10H; diluted 1:500), anti-p63 (4A4; diluted 1:200), anti-p53 (DO-1; diluted 1:5,000), anti-p21WAF (F-5; diluted 1:1,000), anti-MDM2 (Ab-2; diluted 1:1,000), anti-cyclin B1 (V152; diluted 1:1,000), anti- γ H2AX (2577; diluted 1:1,000), anti-Bax (D2E11; diluted 1:1,000), anti-AIF (E1; diluted 1:2,000), anti-GAPDH (6C5; diluted 1:5,000), anti-actin (H-196; diluted 1:2,000) for 2 h at room temperature or overnight at 4 °C.

As secondary antibodies goat-anti-mouse or goat-anti-rabbit IgG HRP-conjugate (diluted 1:5,000–1:10,000) in 3% (w/v) non-fat milk in TBST were used. Peroxidase activity was detected using the Luminol reagent Lite Ablot TURBO (*Euroclone*). Images were acquired using the ChemiDoc (*BIO-RAD*) and the Arbitrary Densitometric Units normalised on those of the GAPDH loading control.

2.7 PARylation in nuclear fraction and on recombinant proteins

Isolated nuclei of MCF7 cells untreated or 1 h treated with TPT 10 μ M were resuspended at 10 mg/ml of proteins in 50 mM Tris-HCl pH 8, containing 10 mM MgCl₂, 1 mM DTT, 0.01% digitonin, 0.1 mM PMSF and a 1:25 dilution of the cocktail of protease inhibitors. Then, were incubated for 30 min at 30 °C with 50 μ M NAD plus 12.5 μ M Bio-NAD.

Alternatively, PARP-1 human recombinant wild-type (200 ng) and [⁹⁸⁸K] mutated (1 μ g) in 50 mM Tris-HCl pH 8, containing 10 mM MgCl₂, 1 mM DTT and after addition of DNase I activated DNA (600 ng) were incubated for 30 min at 30 °C with 1 mM NAD plus 12.5 μ M Bio-NAD in the presence of 5 μ g of recombinant p53.

PARylation reaction was stopped by TCA addition (20% final concentration) and after 15 min standing on ice, the samples were collected by centrifugation at 1,200 x g for 15 min, washed twice with 5% TCA and three times with ethanol.

PARylated proteins were separated by 10% SDS-PAGE, transferred onto a PVDF membrane using an electroblotting apparatus (BIO-RAD) and subjected to immunodetection after blocking with 5% non-fat milk in TBST for 1 hr RT. The following antibodies were used: anti-PARP-1 (C2-10; diluted 1:2,500); anti-p53 (DO-1; diluted 1:5,000); anti-phospho-p53(ser15) (9284; diluted 1:1,000), anti-actin (H-196; diluted 1:2,000), anti-biotin (D5A7; diluted 1:1,000). All antibodies were diluted in 3% non-fat milk in TBST and incubations were for 2 hrs at room temperature or over-night at 4°C. After washing x 3 with TBST, membranes were incubated with peroxidase-conjugated mouse- or goat-anti-rabbit IgG, (diluted 1:5,000-1:10,000) in 3% (w/v) non-fat milk in TBST, for 1 h at room temperature. Finally, membranes were washed three times in TBST and peroxidase activity was detected using the Luminol reagent Lite Ablot TURBO (*Euroclone*). Images were acquired using the ChemiDoc (*BIO-RAD*).

2.8 PAR electrophoretic mobility shift assay

Varying amounts of recombinant p53 were incubated in an appropriate volume of 10 mM Tris-HCl pH 7.4, 1 mM EDTA for 10 min at 25 °C before purified PAR was added and complex formation was allowed to proceed for 20 min at 25 °C to reach equilibrium. Subsequently, the reaction mixture was supplemented with 10x loading dye (0,25% Xylen Cyanol and Bromo phenol Blue, 30% glycerol) resulting in a final volume of 22 µl.

The samples were subjected to a native 5% PAGE for 1.5 h at 160 V and electroblotted onto a nitrocellulose membrane at 260 mA for 1.5 h, followed by a heat-fixation at 90 °C for 1 h. The membrane was then subjected to immunodetection after blocking with 5% non-fat milk in TBST 1 h, with anti-p53 (DO-1; diluted 1:5,000) and anti-PAR (10H; diluted 1:1,000) antibodies and as secondary antibody goat anti-mouse HRP conjugate in 3% non-fat milk in TBST for 1 h at room temperature. Finally, membranes were washed three times in TBST and peroxidase activity was detected using the Luminol reagent Lite Ablot TURBO (*Euroclone*). Images were acquired using the ChemiDoc (*BIO-RAD*).

2.9 Co-Immunoprecipitation

Samples of MCF-7 cells ($1-2 \times 10^6$) untreated or 48 h treated with TPT 2.5 μ M, were resuspended in 50 mM Tris-HCl buffer pH 7.5, containing 150 mM NaCl, 5 mM EDTA, 0.5% NP40, 10% glycerol, 1 mM PMSF and 1:25 dilution of the cocktail of protease inhibitors. Protein A/G plus Agarose was equilibrated in the same buffer by 3 washes and centrifugations at 3,000 rpm 5 min at 4 °C: 40 μ l aliquots were incubated with 1 mg of protein extract in 1 ml final volume, by buffer addition. Anti-p53 (DO-1), anti PARP-1 (C2-10) or anti-PAR (4335) monoclonal antibodies were added (3 μ l) and the suspensions were incubated overnight at 4 °C under constant agitation.

Co-immunoprecipitated samples were washed 3 times with the same buffer, mixed 1:1 with 4x Laemmli Buffer and, together with total protein extracts (30 μ g), were subjected to 10% SDS PAGE, transferred onto a PVDF membrane using an electroblotting apparatus (*BIO-RAD*) and subjected to immunodetection, after blocking with 5% non-fat milk in TBST for 1 h, with anti-PARP-1 (9542; diluted 1:1,000) and anti-p53 (FL-393; diluted 1:5,000) antibodies.

3. Results Section 1: p63 involvement

3.1. Effect of PJ34 on CPT/TPT-induced growth inhibition and cell cycle distribution in human carcinoma cells

Preliminary experiments, in breast carcinoma MCF7^{p53wt} cells, showed that 1 μ M CPT inhibits cell growth similarly to 5 μ M TPT. To potentiate the CPT/TPT cytostatic effect, PJ34 concentrations were used in a sub-lethal range (10–20 μ M). A 48 h of exposure, corresponding approximately to two rounds of MCF7^{p53wt} cell replication, was used according to the administration procedure during anticancer therapy. As shown in **Figure 6**, at 24 h CPT/TPT treatment has a cytostatic effect, while PJ34 induces growth retardation in a dose-dependent way, whereupon cells start to recover but the rate of recovery was significantly affected by CPT-PJ34 combined treatment.

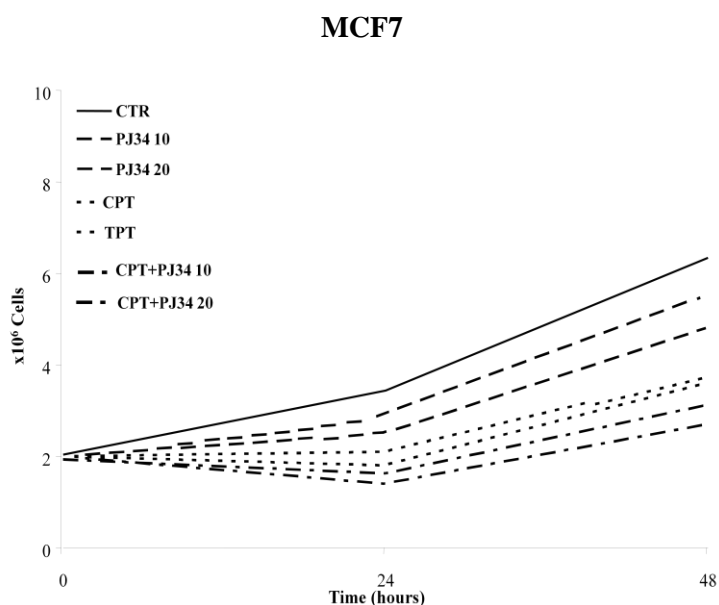


Figure 6. Dose-dependent response of MCF7 cells treated with CPT/TPT and PJ34 as single agents or in combination.

MCF7 were treated for 24–48 h with CPT 1 μ M or TPT 5 μ M and 10 or 20 μ M PJ34 alone or in combination: cell growth was measured by cell counting at different time points. Data refer to at least three experiments giving similar results.

Results

We next investigated the impact of CPT on MDA-MB231 and SCC022 cell survival. MDA-MB231 express a mutant p53 (p53R280K) while SCC022 cells are p53 null. Cells were plated, treated with CPT 1 μ M for 48 h and subjected to the MTT assay to compare viability of treated and untreated cells. As shown in **Figure 7**, CPT significantly reduces cell viability of all cell lines tested (around 50% of control). Moreover, treatment with PJ34 alone affects MCF7 and MDA-MB231 cell viability, in a dose-dependent way, whereas SCC022 cells remain almost unaffected. Interestingly, compared with single drug treatments, combination of PJ34 with CPT results in a significant enhancement of cytotoxicity in MCF7 cells (37–33% of cell survival) while in MDA-MB231 and SCC022 cells addition of PJ34 to CPT has a lower impact on cell survival. Each plot represents the media of triplicates from three independent experiments \pm S.E. Similar results are observed when PJ34 is added to TPT (data not shown).

MTT ASSAY

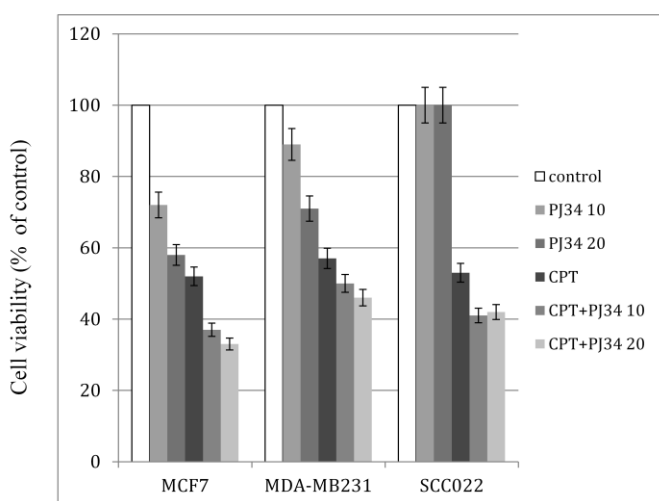


Figure 7. Cell growth inhibition in MCF7, MDA-MB231 and SCC022 cells treated with CPT and PJ34 as single agents or in combination.

Cells (10^4 cells/plate) MCF7, MDA-MB231 and SCC022 48 h treated were used for determination of cell growth inhibition by MTT assay. Each plot represents the media of triplicates from three independent experiments \pm S.E.

Results

We have previously reported that TPT at concentrations higher than 1 μM promptly arrested the cells in S phase, while concentrations equal or lower than 1 μM cause a G2/M arrest (*D'Onofrio et al; 2011*). To gain insight into the molecular mechanism of TPT-PJ34 interactive cytotoxicity, we analysed the cell cycle distribution of MCF7 cells treated with 10 or 20 μM PJ34 alone or in combination with 1 μM TPT. As shown in **Figure 8**, after 48 h treatment, 1 μM TPT as well as 10 or 20 μM PJ34 induce accumulation of cells in G2/M phase and the cell cycle distribution is less affected by treatment with PJ34 (10 or 20 μM) than TPT used as single agents. The difference in G2% of cells between PJ34 10 or 20 μM is considered not significant as sublethal doses. Furthermore, addition of 10 or 20 μM PJ34 to 1 μM TPT causes a significant increase of G2/M cells, while S-phase cells are drastically reduced. **Figure 8 (table)** also shows that single treatments cause an increase of cells with a sub-G1 DNA content (from 6 to 19%), probably due to induction of apoptotic cell death. Remarkably, an increase up to 55% of sub-G1 cells is observed with TPT 1 μM + PJ34 20 μM combined treatment, showing a 2x potentiation factor of PJ34 on TPT cytotoxicity.

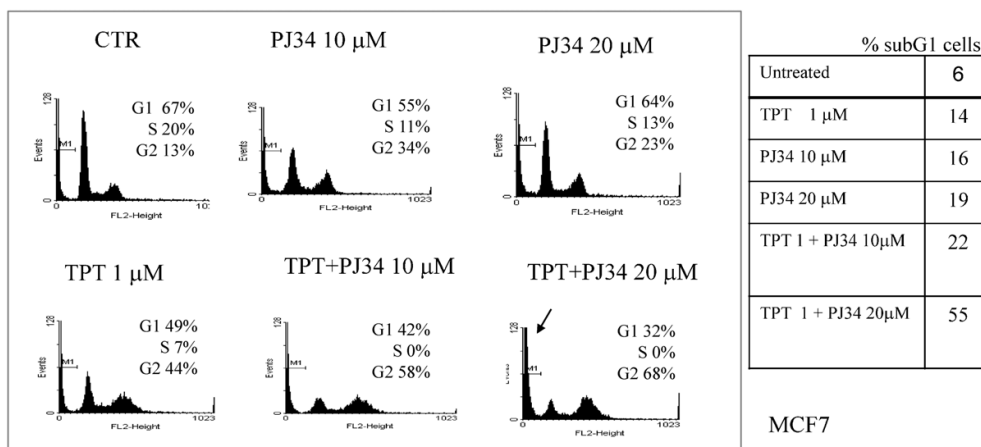


Figure 8. Cell cycle analysis of MCF7 cells subjected to TPT and PJ34 single and combined treatments.

MCF7 cells were treated 48 h with TPT 1 μM and 10 or 20 μM PJ34 alone or in combination. Control and treated cells (1×10^6) were fixed in 70% ethanol and used for flow cytometric analysis (see Section 2). Determination of DNA content after PI staining is shown and cells in G1, S and G2 phase are indicated as percentage (excluded sub-G1 cells). The table reports sub-G1 cells as the percentage of the entire population of cells. Data refer to one of three experiments giving similar results.

3.2. Analysis of CPT- or TPT-dependent TOP 1 inactivation

It is already known that CPT and TPT abolish the religation activity of TOP 1 generating an abortive complex to which the enzyme is covalently linked (*Pommier et al; 2006*). Therefore, we determined the efficacy of TOP 1 inhibitors by looking at their capacity of trapping the enzyme in the abortive complex. This was detected, by looking at the disappearance of the immunoreactive band of the TOP 1 soluble fraction by western blot analysis. After 48 h of treatment, both 1 μM CPT and 5 μM TPT are able to block, almost completely, the TOP 1 enzyme in the abortive complex, in all cell lines tested (**Figure 9**). According to previous findings (*D'Onofrio et al; 2011*), PJ34 does not affect TOP 1 enzyme trapping when used in combination with CPT or TPT.

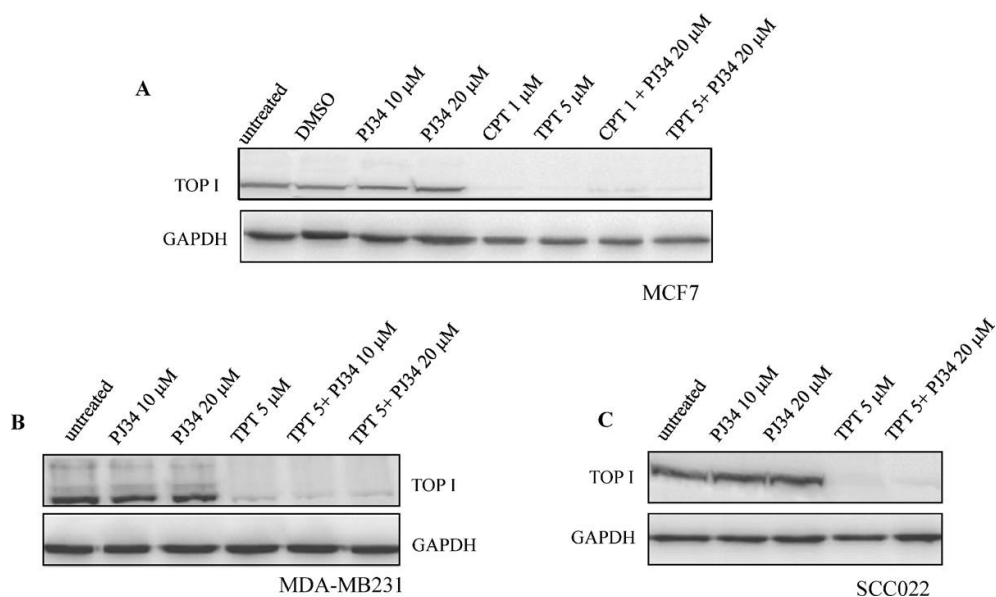


Figure 9. Western blot analysis of TOP 1 soluble fraction in carcinoma cells untreated or 48 h treated with the indicated drugs.

Untreated and treated whole cell extracts (50–100 μg of proteins) were subjected to 10% SDS-PAGE, electroblotted on PVDF and incubated with the anti-TOP 1 antibody. Immunodetection in MCF7 (**A**), MDA-MB231 (**B**) and SCC022 (**C**) cells is shown. 0.1% DMSO treated cells were analysed as CPT internal control. GAPDH was used as loading control.

3.3. Analysis of PAR synthesis in carcinoma cells after treatment with TPT ± PJ34

PJ34 efficacy as PARP inhibitor was assessed by looking at its effect on PARP-1 automodification. Proliferating MCF7 cells were exposed to the drugs and samples were then analysed by SDS-PAGE. As shown in **Figure 10**, the identity of the PAR modified protein was detected by western blotting using a PARP-1 antibody showing a mobility shift of the immunoreactive band at the top of the gel (**Figure 10A, lane 4**). Such a behaviour indicates auto-modification of PARP-1 by long and branched ADP-ribose polymers (up to 200 residues in chain) on several sites (up to 25) of the auto-modification domain. This process gives rise to higher molecular weight PARP-1 forms that do not enter the polyacrylamide gel matrix. Interestingly, TPT–PJ34 co-treatment in MCF7 cells induced apoptosis as demonstrated by the appearance of the 89 kDa fragment generated by the caspase-dependent cleavage of PARP-1 (**Figure 10A, lanes 5 and 6**).

Furthermore, we analysed the response of SCC022 squamous carcinoma cells to PJ34 and TPT treatment. Immunoblot with the PARP-1 specific antibody reveals that PARP-1 is modified since the unmodified 113 kDa band is strongly reduced (**Figure 10B, lane 4**). PJ34 co-treatment drastically reduces TPT-induced PARP-1 auto-modification thus leading to the accumulation of the 113 kDa band of PARP-1. However, we did not observe PARP-1 specific cleavage, thereby suggesting that cells were not undergoing apoptosis (**Figure 10B, lanes 5 and 6**).

Immunoblot analysis with PARP-1 antibody was also performed in MDA-MB231 cells subjected to the same treatments. As shown in **Figure 10C**, in TPT-treated cells PARP-1 is auto-modified at a lower extent (**lane 4**) and there are no signs of apoptosis induction after TPT-PJ34 combined treatment (**Figure 10C, lanes 5 and 6**).

All together, our results suggest that, compared to MCF7, SCC022 and MDA-MB231 cells are less sensitive to the drugs combination and do not respond immediately with apoptosis to TOP 1 and PARP-1 inhibitors co-treatment.

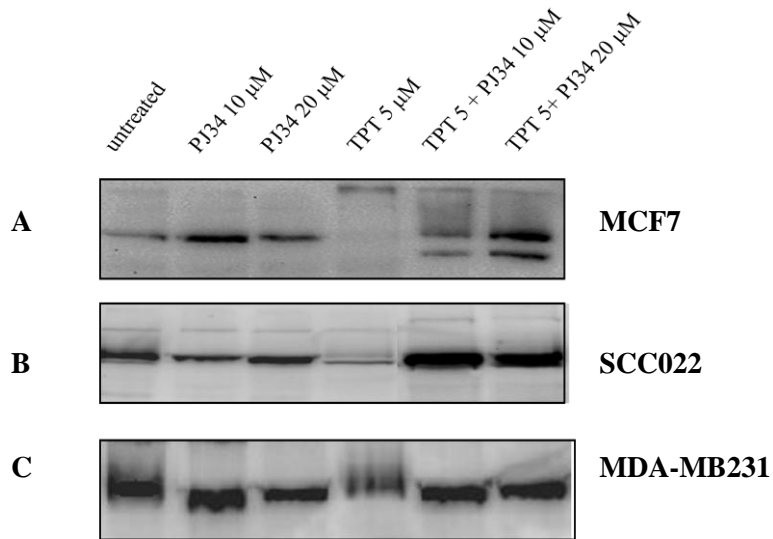


Figure 10. Analysis of TPT-dependent PARP-1 activation or PJ34-dependent PARP-1 inhibition in carcinoma cells untreated or 48 h treated with the indicated drugs.

Whole cell extract (50-100 μ g of proteins) after 10% SDS-PAGE and electroblotting on PVDF were incubated with anti-PARP-1 antibody. Immunodetection of PARP-1 in whole cell protein extract from untreated and treated MCF7 (A), SCC022 (B) and MDA-MB231 (C) cells is shown.

3.4. Involvement of p63 in the cell response to TPT ± PJ34 treatment

To get insight into the molecular mechanism underlying the response of MCF7 cells to TPT ± PJ34 treatment, we analysed the expression of p53, p63 and other cell cycle and apoptosis markers such as p21WAF, MDM2 and cyclin B1. In MCF7 cells we found that PJ34 addition to TPT strongly enhances the TPT-dependent stimulation of p53 expression. Remarkably, the p53 negative regulator MDM2 was down-regulated only upon combined treatment. Furthermore, using the 4A4 monoclonal antibody which recognizes all p63 isoforms, we only detected bands corresponding to the pro-apoptotic TAp63 α and γ isoforms; both isoforms are up-regulated by TPT–PJ34 co-treatments (**Figure 11A**).

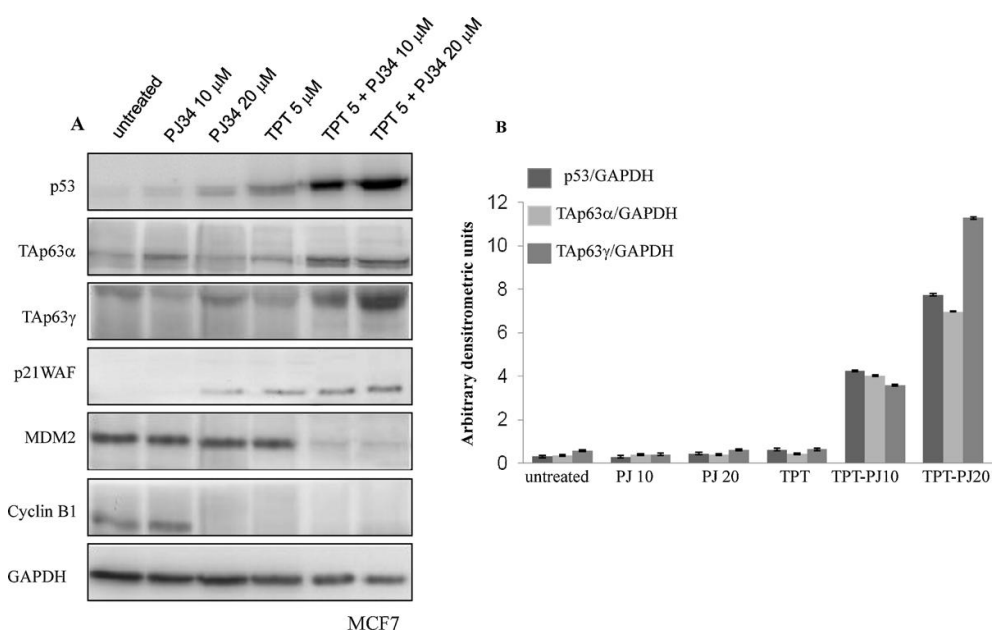


Figure 11. Western blot analysis of p53, p63, p21WAF, MDM2 and cyclin B1 expression in MCF7 cells untreated or 48 h treated with the indicated drugs.

Whole cell extract (50–100 μ g of proteins) after 10% SDS-PAGE and electroblotting on PVDF were incubated with the different antibodies. (A) Immunodetection of p53, p63, p21WAF, MDM2, cyclin B1. GAPDH was used as loading control; (B) p53 and TAp63 α and γ band intensities were quantified by densitometric scanning. Data expressed as Arbitrary Densitometric Units (ADU) were normalized to the internal control GAPDH. Shown are the mean of three different experiments \pm S.E.

Results

Quantitation of proteins by densitometric scanning, reveals a 19–20-fold increase of the expression level for both p53 and p63 proteins after TPT–PJ34 20 μ M treatment (**Figure 11B**). The increase of p21WAF expression level was concomitant to a decrease of cyclin B1 thereby supporting the G2/M cell cycle arrest observed by cytofluorimetric analyses.

We also performed immunoblot analysis of MCF7 nuclear and cytoplasmic fractions. **Figure 12A** shows that following TPT \pm PJ34 treatment both p53 and TAp63 γ accumulate in the nuclear compartment. Nuclear γ H2AX expression and PARP-1 specific cleavage were monitored as markers of dsDNA damage and caspase-dependent apoptosis, respectively (**Figure 12A**). Furthermore, the expression level of the pro-apoptotic BAX protein, whose gene is transcriptionally activated by p53 and TAp63, increases in the cytoplasmic fraction by either TPT alone or TPT–PJ34 combined treatment, while the level of the mitochondrial apoptosis inducing factor AIF is unaffected (**Figure 12B**).

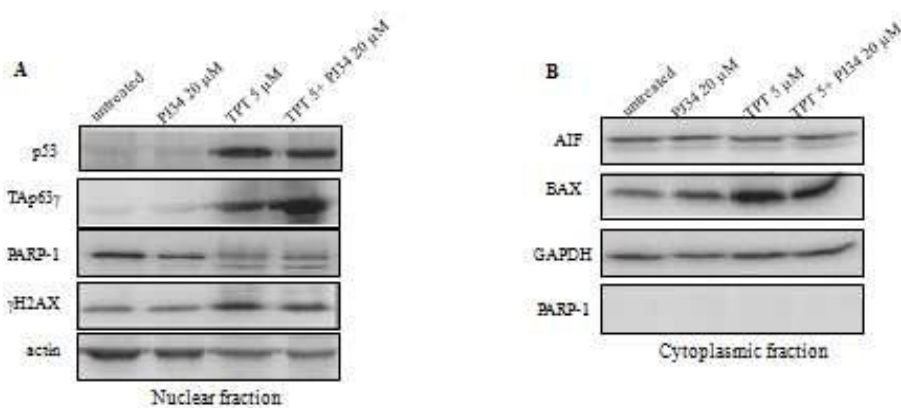


Figure 12. Western blot analysis of protein extract from nuclear and cytoplasmic fraction of MCF7 cells untreated or 48 h treated with the indicated drugs.

Whole extract (50–100 μ g of proteins) after SDS-PAGE and electroblotting on PVDF were incubated with the different antibodies. Immunodetection of p53, p63, PARP-1, γ H2AX, BAX, AIF in nuclear (A) and cytoplasmic (B) fractions from MCF7 cells. Actin and GAPDH were used as loading controls, respectively.

Results Section 2: p53 PARylation

3.5 PARylation in isolated nuclei

Nuclei were isolated from MCF7 cells untreated or 1 h treated with TPT 10 μ M. Protein extracts were subjected to western blot analyses to determine functional changes in PARP-1 and p53 as a consequence of the treatment. **Figure 13A** shows in the untreated sample a PARP-1 immunoreactive band that in the TPT treated sample was split in widespread components. Such phenomenon is a consequence of the electrophoretic mobility shift determined by the auto-modification of PARP-1 by PAR chains of different length. Furthermore, the amount of the 89 kDa PARP-1 apoptotic fragment increased following the treatment. We also observed the TPT-dependent nuclear accumulation of p53 which was phosphorylated at serine15 residue, a sign of DNA damage (**Figure 13A**).

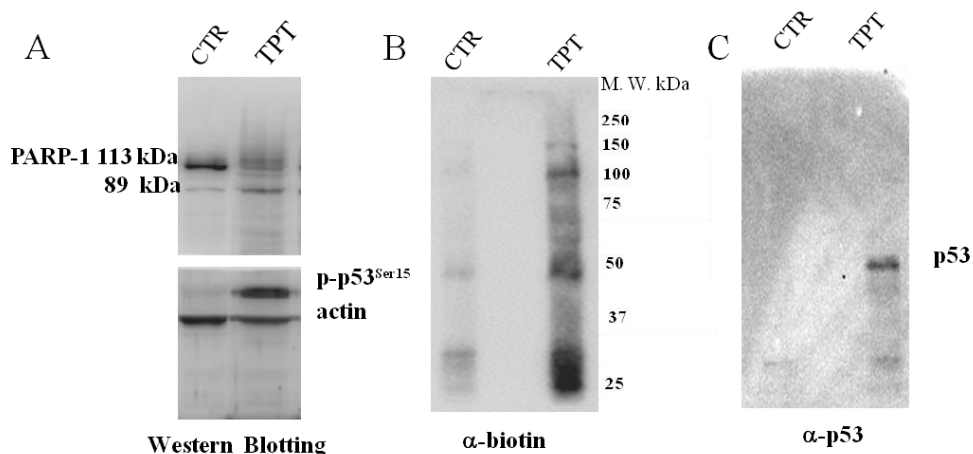


Figure 13. Western blot analyses of nuclei isolated from MCF7 cells untreated or 1 h treated with TPT 10 μ M.

Whole nuclear extracts (~ 100 μ g of proteins) were subjected to 10% SDS-PAGE, electroblotted on PVDF and incubated with anti-PARP-1, anti p-p53^{Ser15} and anti-actin antibodies (**A**) or previously incubated with a NAD plus Bio-NAD mixture and incubated with anti-biotin antibody (**B**) and anti-p53 antibody (**C**).

An aliquot of nuclei isolated from untreated and treated MCF7 cells was then incubated with NAD and biotinylated NAD (Bio-NAD) and PARylated proteins were identified by immunological analyses using an anti-biotin antibody. The anti-biotin immunodetection in **Figure 13B** shows a strong

Results

induction of Bio-PAR synthesis associated with several nuclear components in TPT treated nuclei. Immunoreactive bands near the top of the gel can likely be ascribed to auto-modified forms of PARP-1, while that at the bottom of the gel to PARylated histones. Furthermore, the anti-biotin immunoreactive band in correspondence of the 50 KDa MWM, was identified by a subsequent immunodetection with an anti-p53 antibody (**Figure 13C**), thereby showing that p53 can be one of the PAR target/acceptor proteins in this experimental setting.

3.6 *In vitro* p53 PARylation

To better define the mechanism of p53 PARylation we set-up an *in vitro* assay by the use of recombinant p53 protein, PARP-1^{wild type} and a PARP-1^{E988K} mutant enzyme which lacks the ability of ADP-ribose elongation and branching (Rolli *et al.*; 1997). Both PARP-1^{wild type} and PARP-1^{E988K} were incubated with a NAD plus Bio-NAD mixture in the presence of 5 µg of p53.

In **Figure 14A** coomassie stained bands are shown for PARP-1^{E988Kmut} and p53, while PARP-1^{WT} was not seen as it is spread in its multiple auto-modified forms. Moreover, anti-biotin immunodetection demonstrates that PARP-1^{E988K} mutant was auto-modified by mono-ADP-ribose as known for such a form of the enzyme. Furthermore, as shown in **Figure 14B**, anti-biotin immunoreactive bands were evidenced (indicated by asterisks) in correspondance to the coomassie stained p53 band or slightly retarded by incubation with PARP-1^{WT}.

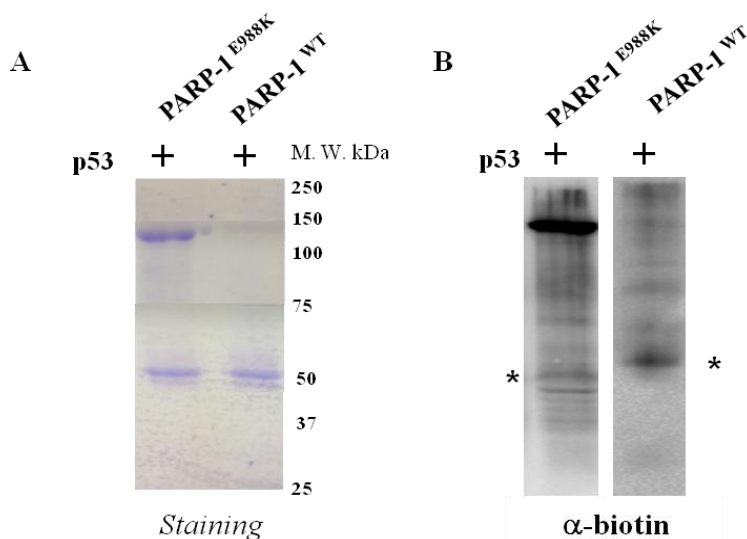


Figure 14. *In vitro* PARylation assays.

Human recombinant PARP-1^{WT} (200 ng) and PARP-1^{E988K} mutated (1 µg) were incubated with a NAD plus Bio-NAD mixture in the presence of 5 µg of human recombinant p53. Protein samples were subjected to 10% SDS-PAGE and electroblotted on PVDF.

A: coomassie stained bands on PVDF membrane; **B:** anti-biotin immunodetection.

Results

To analyse PAR p53 non-covalent interaction we performed a PAR electrophoretic mobility shift assay. **Figure 15 panel A** shows immunodetection of increasing amount recombinant p53 (1 - 4 μg) incubated with PAR ($\sim 1 \mu\text{g}$) and subjected to 5% native PAGE and blotting on nitrocellulose filter; **panel B** shows the anti-PAR immunodetection of the same filter confirming the presence of the p53 protein in complexes with PAR. Free PAR was not detected since nitrocellulose membrane does not bind it (*Malanga et al; 1998*).

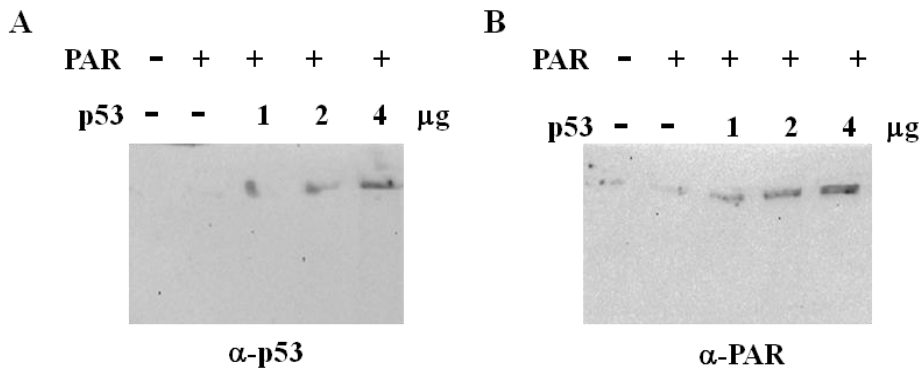


Figure 15. PAR EMSA.

Purified PAR was incubated with different aliquots of recombinant p53 and subjected to native 5% PAGE, blotting on nitrocellulose and immunodetection of PAR-proteins complexes with anti-p53 (**A**) and anti-PAR (**B**) antibodies.

3.7 p53 PARylation in TPT treated MCF7 cells.

The p53 PARylation deriving from TOP 1 inhibition-dependent DNA damage in MCF7 cells was evidenced by co-immunoprecipitation experiments. Aliquots of MCF7 lysates, after 48 h treatment with TPT 2.5 μ M, were subjected to anti-p53, anti PARP-1 or anti-PAR immunoprecipitations, followed by anti-PARP-1 and anti-p53 immunodetection.

Figure 16 panel A shows the presence of three major anti-PARP-1 immunoreactive bands corresponding to the native enzyme (113 kDa), to its auto-modified forms (PAR-PARP-1) and to the 89 kDa apoptotic fragment both in the input sample and in the anti-PARP-1 immunoprecipitates. Interestingly, only the band corresponding to the auto-modified form of PARP-1 was evidenced in the p53 immunoprecipitated sample. Immunoprecipitation with an anti-PAR antibody is shown to confirm the identification of PARylated PARP-1.

Furthermore, **Figure 16 panel B**, shows that the p53 immunoreactive band of the input sample is also present both in anti-p53 and anti-PAR immunoprecipitated samples. Samples immunoprecipitated with an irrelevant IgG control are also shown (**Figure 16, panel C**).

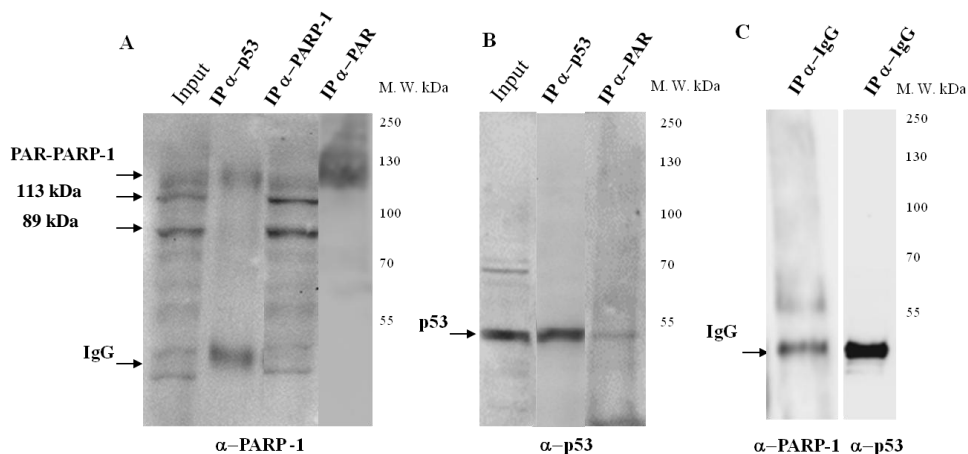


Figure 16. Western blot analyses of co-immunoprecipitation of MCF7 cells 48 h treated with TPT 2.5 μ M.

Whole cell extract (input) and samples immunoprecipitated with anti-p53 (DO-1), anti-PARP-1 (C2-10) or anti-PAR (4335) antibodies, after 10% SDS-PAGE and electroblotting on PVDF membrane, were subjected to immunodetection with anti-PARP-1 (9542) (**panel A**) and anti-p53 (FL-393) antibodies (**panel B**). Immunodetections of irrelevant IgG immunoprecipitated samples are also shown (**panel C**).

Results Section 3: Involvement of PARP inhibitors in the p53/p63 signaling pathway

With this aim we analysed p53 null SCC022 cells that are known to express the Δ Np63 α isoform, required for the survival of SCC cells (Devy *et al.*; 2004). Furthermore, we compared cells transfected with p53 and/or p63 and subjected to TPT \pm PJ34 treatment.

Figure 17 shows the results of immunological analyses of SCC022 cell subjected to 24 hours treatment with 5 μ M TPT \pm 20 μ M PJ34 compared with the same cells previously transfected with p53.

In **Panel A** the TPT-dependent PARP-1 auto-modification is evident since the immunoreactive band is spread in its multiple auto-modified forms (**lane 3** PAR-PARP-1) while a band in correspondance of the native enzyme (**lane 4** PARP-1 113 kDa) is the consequence of PJ34 addition.

Furthermore, Δ Np63 α expression level is dramatically down-regulated by TPT treatment with or without PJ34. Concomitantly, cyclin B1 appears to be reduced while p21 is stimulated by TPT treatment with or without PJ34, suggesting a G2/M cell cycle arrest.

Panel B shows the same analysis performed in cells transfected with p53 (**lanes 2 and 4**) before TPT+PJ34 treatment. Interestingly, we observed that the TPT \pm PJ34 dependent Δ Np63 α down-regulation was not sufficient to induce caspase-dependent apoptosis, but p53 transfection was necessary as shown by the appearance of the PARP-1 89 kDa apoptotic fragment (**lane 4**).

Importantly, using an anti-p63 antibody (4A4), we were unable to detect p63 isoforms other than Δ Np63 α both in untreated and TPT \pm PJ34 treated SCC022 cells (data not shown).

Therefore we subjected to the same analyses cells transfected with the pro-apoptotic isoform TAp63 γ .

Figure 18 shows the results of immunological analyses of SCC022 cells transfected with p53 and TAp63 γ alone or together, and subjected to 5 μ M TPT + 20 μ M PJ34 combined treatment.

Immunodetection with the anti-p53 antibody confirmed the ectopic expression of such protein. Furthermore, with the anti-p63 antibody, we were able to detect, beside the immunoreactive band corresponding to the endogenous Δ Np63 α isoform, a weak band ascribed to the ectopically expressed TAp63 γ . Interestingly, as for the PARP-1 immunodetection, the 89 kDa apoptotic fragment became evident as a consequence of TAp63 γ \pm p53 transfection. Moreover, BAX expression was observed in the same samples as a marker of apoptosis induction.

In conclusion, we confirmed also in squamous carcinoma cells a p53-dependent apoptosis induction as a consequence of PARP-1 inhibition.

Results

Moreover we got evidences that, the change of cell fate can be related to the switch from the Δ Np63 α anti-apoptotic isoform to the TAp63 γ pro-apoptotic isoform expression.

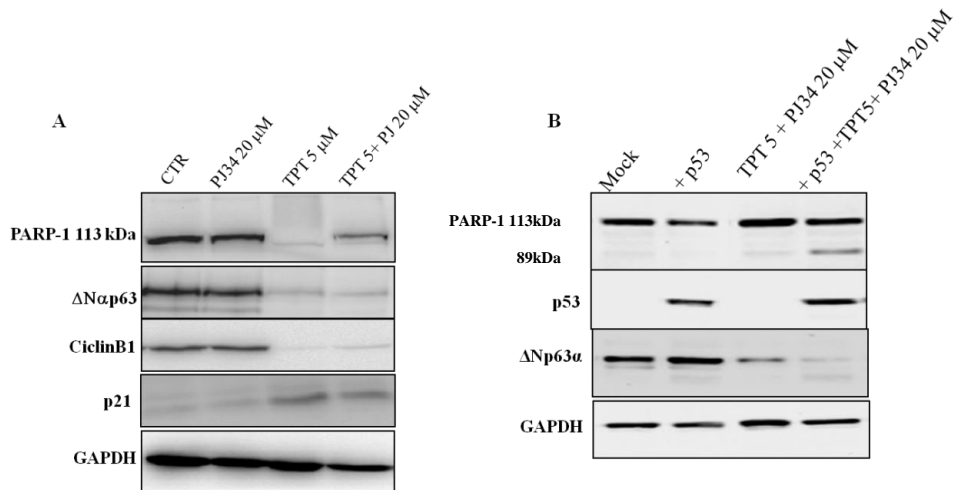


Figure 17. Western blot analysis of protein extract from SCC022 cells untreated or treated with TPT \pm PJ34 before and after p53 transfection.

Untreated and treated whole cell extracts (50–100 μ g of proteins) (A), transfected or not with p53 (B) were subjected to 10% SDS-PAGE, electroblotted on PVDF and incubated with different antibodies. Immunodetection of PARP-1, Δ Np63 α , p53, cyclin B1 and p21 is shown. GAPDH was used as loading control.

Results

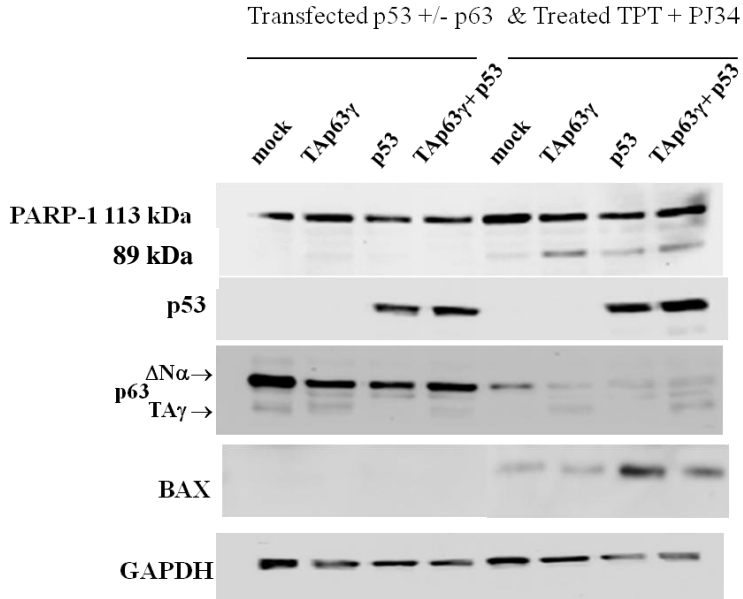


Figure 18. Western blot analysis of protein extract from SCC022 cells transfected for p53 and/or TAp63 γ and treated with TPT + PJ34.

Whole cell extracts (50–100 μ g of proteins) from mock and p53/TAp63 γ transfected cells, after 24 h treatment with 5 μ M TPT and 20 μ M PJ34, were subjected to 10% SDS-PAGE, electroblotted on PVDF and incubated with different antibodies. Immunodetection of PARP-1, p63, p53 and BAX is shown. GAPDH was used as loading control.

4. Discussion

The efficacy of PARP inhibitors as chemosensitizers has led to the development of a multitude of such molecules with different bioavailability and pharmacokinetic properties that are currently under investigation in clinical trials (*Rouleau et al; 2010*). However, a clear understanding of how PARP inhibitors potentiate the activity of antineoplastic agents is still lacking.

The hydrophilic PARP inhibitor PJ34 has already been reported to synergize with cisplatin- and TPT-dependent apoptotic induction in triple-negative breast cancer and human carcinoma cells expressing wild type p53 (*Hastak et al; 2010*). We have already shown that PJ34, at a concentration of 5 μ M, inhibits PARP-1 activity without cytotoxic effects. Furthermore, in HeLa and MCF7 cells we found that TPT toxicity was higher when PAR synthesis was reduced by either PARP-1 silencing or PJ34 administration (*D'Onofrio et al; 2011*).

In the present study, we compared the response of MCF7^{p53wt}, MDA-MB231^{p53mut} and SCC022^{p53null} cells to treatment with higher concentration of PJ34 (up to 20 μ M) in combination with 1 μ M CPT or 5 μ M TPT. According to the previously reported specificity of PARP inhibitors for breast cancer (*Bryant et al; 2005*), we observed a higher sensitivity to PJ34 in MCF7^{p53wt} cells. In such cells we confirmed that TPT, which is known to be S-phase specific (*Feeney et al; 2003*), causes a G2/M cell cycle arrest when used at a lower concentration (1 μ M). In addition, the TPT-dependent G2/M cell cycle arrest was enhanced by TPT + PJ34 combined treatment and resulted in a remarkable increase of cells with sub-diploid DNA, confirming a synergic cytotoxic effect of TOP 1 and PARP-1 inhibitors.

Consistent with the idea that poly(ADP-ribosyl)ation plays a role in the response to CPT/TPT-induced DNA damage, we observed the disappearance of a TOP 1 soluble/active fraction and the PARP-1 auto-modification in MCF7, MDA-MB231 and SCC022 cells thereby indicating that the response to DNA damage, induced by TOP 1 inhibitors, in skin squamous carcinoma cells is similar to that observed in breast carcinoma cells (*Davis et al; 1998*).

On the other hand, we found that prevention of PARP-1 auto-modification by PJ34 induces PARP-1 proteolysis only in MCF7^{p53wt} implying that apoptosis induced by inhibition of PAR synthesis requires the p53 wild type activity.

Given the similarity between p53 and p63, it was of interest to look at the effect of TOP 1 + PARP-1 inhibitors on p63 protein isoforms. Interestingly, TPT + PJ34 treatment in MCF7 cells causes a remarkable increase of TAp63 α and γ protein levels. TAp63 γ in particular, was reported to be a potent apoptosis inducer (*Yang et al; 1998*). Both p53 and TAp63 γ accumulated in

the nuclear fraction where the proteins could functionally interact in the control of transcription. Consistently, TPT + PJ34 combined treatment caused a dramatic reduction of MDM2, a negative regulator of p53 transcriptional activity and protein level. Remarkably, this is the first evidence of a PJ34-inducible proapoptotic response involving both p53 and p63 family members in breast carcinoma cells.

Furthermore, in SCC022^{p53null} cells we showed that CPT/TPT single or combined treatments suppressed the endogenously expressed Δ Np63 α anti-apoptotic isoform together with cyclin B1. It has previously been demonstrated that Δ Np63 α is required for the survival of SCC cells by virtue of its ability to suppress p73-dependent apoptosis (*Rocco et al; 2006*). However, TPT + PJ34 treatment is not sufficient to induce apoptosis in these cells, thereby suggesting either the presence of a non-functional p73 or the existence of an alternative anti-apoptotic pathway able to overcome Δ Np63 α depletion. Similarly, it has been reported that in MDA-MB468 cells expressing high level of Δ Np63 α , PJ34 reduced Δ Np63 α level, with a concomitant increase of p73. Interestingly, in SCC022 cells p53 transfection is necessary to induce cell detachment and apoptosis after TPT-PJ34 combined treatment.

Therefore, it can be postulated that carcinoma cells, depending on their genetic background (p53/p63 null versus p53/p63 proficient), can trigger a p53-dependent pathway to induce cell cycle arrest and apoptosis, as a results of concomitant inhibition of PARP-1 and TOP 1. To this respect, the particular p63 isoform expressed may sustain (TAp63 α and γ) or inhibit (Δ Np63 α) the execution of the apoptotic program.

We have identified p63 as a new player of the PARP-1-dependent signaling of DNA damage. Interestingly, in the p63 DNA binding domain, both the PAR binding motif and the glutamic acid residues showed to act as covalent PAR acceptor sites are conserved.

Our findings contribute to the understanding of the molecular events triggered by TOP 1 and PARP-1 inhibitor-dependent genomic damage and provide a rationale for the development of new approaches to sensitize cancer cells to chemotherapy.

A yet unsolved problem is the discrimination between covalent and non-covalent modification of proteins by PAR. It has already been shown (*Malanga et al; 1998*) a non-covalent interaction between PAR and purified or recombinant proteins such as histone H1 and p53, blotted on nitrocellulose membrane. Indeed, PAR binding motifs have been identified in several proteins included H1 and p53 (*Krietsch et al; 2013*). Furthermore, covalent hetero-modification sites have been identified on histones by proteomic approach (*Messner et al; 2010*) and p53 by the analysis of deletion mutants (*Kanai et al; 2007*).

Following DNA damage, the synthesis of PAR participates in the induction of p53 and for consequence in the expression of p53-responsive genes. In fact, p53 functions are impaired in cells exposed to PARP inhibitors (Valnezuela *et al*; 2002).

We have previously shown that, in response to DNA damage, TPT induces p53 over-expression in MCF7 breast carcinoma cells thus leading to a G2/M cell cycle arrest.

Here we have investigated on the mechanism underlying PARP-1 physical and functional interaction with p53 in the signaling of TPT-dependent DNA damage. With this purpose, we first determined the nuclear co-localization of an auto-PARylated form of PARP-1 and a phosphorylated form of p53 at serine 15 residue, that are known to represent activated forms of PARP-1 and p53 protein, respectively (Ray *et al*; 2012).

Furthermore, we performed both *in vitro* and *in cell* analyses aimed at the definition of the p53 PARylation mechanism.

Herein, we have identified p53 as a possible target or acceptor of the high amount of PAR synthesized in nuclei of MCF7 cells subjected to TOP 1 inhibitor treatment. Free PAR deriving from PARG endoglycosidic cleavage of PARylated PARP-1 might be present in the nuclei. Indeed, it has been reported that free PAR can reach the mitochondria where it binds apoptosis-inducing factor (AIF) (Wang *et al*; 2011).

To discriminate between covalent or non-covalent PARylation we set-up an *in vitro* enzymatic assay and a PAR-EMSA. However, from these approaches, we draw indications that p53 could act either as a substrate of hetero-modification reaction catalyzed by recombinant PARP-1 and as a free PAR interacting protein.

Such evidences can be matched considering that PAR polymers exhibit a high negative charge (2 for each ADPribose unit, double that of DNA), that allows them to easily interact with nuclear proteins (i.e. p53).

Nevertheless, *in vitro* approaches as test tube conditions are unlikely to mirror the situation in the cells. Therefore, we used co-immunoprecipitation experiments in DNA damaged MCF7 cells and we observed that PAR, covalently linked to PARP-1, interacts with p53.

This observation highlights a molecular mechanism by which the polymers clustered on PARP-1 at DNA breakage sites could affect the activation of p53 and/or interfere with its transcriptional function, in response to different levels of DNA damage (Malanga *et al*; 2005).

Moreover, in our experimental setting, we have evidenced that PAR covalently bound to PARP-1 may induce ^{ser15}p-p53 accumulation in the nucleus, suggesting that a possible mechanism through which PARylation could modulate p53 transactivation activity is by contributing to p53 nuclear

retention and/or stabilization. As a consequence, the expression of target genes as p21, cyclin B1 is stimulated in a DNA repair attempt. On the other hand, PARP inhibitors stimulate the expression of pro-apoptotic genes (i.e. BAX).

Interestingly, p63 has been identified as a co-player of this PARP-1-dependent signaling of DNA damage. In the p63 DNA binding domain, the PAR binding motifs determined in p53 are conserved (*Malanga et al; 1998*).

In conclusion these findings contribute to the understanding of the molecular events triggered by TOP 1 and PARP-1 inhibitor-dependent genomic damage.

In particular, evidences were got that PARP-1 inhibitors can act to overcome the apoptotic threshold determined by expression level of p53 family proteins in different cellular contexts, which have important implications for the effectiveness of p53-based cancer therapy.

5. References

- Beneke, S. (2012). Regulation of chromatin structure by poly(ADP-ribosylation). *Front. Genet.* 3, 169.
- Bryant, H.E., Schultz, N., Thomas, H.D., Parker, K.M., Flower, D., Lopez, E., et al. (2005). Specific killing of BRCA2-deficient tumours with inhibitors of poly(ADP-ribose) polymerase. *Nature* 434(7035), 913.
- Cazzalini, O., Dona', F., Savio, M., Tillhon, M., Maccario, C., Perucca, P., et al. (2010). p21CDKN1A participates in base excision repair by regulating the activity of poly(ADP-ribose) polymerase. *DNA Repair* 9(6), 627–35.
- Chan, W.M., Siu, W.Y., Lau, A., Poon, R.Y. (2004). How many mutant p53 molecules are needed to inactivate a tetramer? *Mol Cell Biol.* 24(8), 3536-51.
- Cimmino, G., Pepe, S., Laus, G., Chianese, M., Prece, D., Penitente, R., et al. (2007). Poly(-ADPR)polymerase-1 signaling of the DNA damage induced by DNA topoisomerase I poison in D54(p53 wt) and U251(p53mut) glioblastoma cell lines. *Pharmacol. Res.* 55(1), 49–56.
- Dai, C., and Gu, W. (2010). p53 post-translational modification: deregulated in tumorigenesis. *Trends Mol. Med.* 16(11), 528–536.
- Davis, P.L., Shaiu, W.L., Scott, G.L., Iglehart, J.D., Hsieh, T.S., Marks, J.R. (1998). Complex response of breast epithelial cell lines to topoisomerase inhibitors. *Anticancer Res. J.* 18(4C), 2919–32.
- De Laurenzi, V., Melino, G. (2000). Evolution of functions within the p53/p63/p73 family. *Ann N Y Acad Sci.* 926, 90–100.
- Devy, J., Wargnier, R., Pluot, M., Nabiev, I., Sukhanova, A. (2004). Topotecan-induced alterations in the amount and stability of human DNA topoisomerase I in solid tumor cell lines. *Anticancer Res.* 24(3a), 1745–51.
- Di Costanzo, A., Festa, L., Roscigno, G., Vivo, M., Pollice, A., Morasso, M., et al. (2011). A dominant mutation etiologic for human Tricho-Dento-Osseus syndrome impairs the ability of DLX3 to downregulate $\Delta Np63\alpha$. *J. Cell. Physiol.* 226(8), 2189–97.
- Di Costanzo, A., Troiano, A., di Martino, O., Cacace, A., Natale, C.F., Ventre, M., et al. (2012). The p63 Protein Isoform $\Delta Np63\alpha$ Modulates Y-box Binding Protein 1 in Its Subcellular Distribution and Regulation of Cell Survival and Motility Genes. *J. Biol. Chem.* 287(36), 30170–80.
- D'Onofrio, G., Tramontano, F., Dorio, A.S., Muzi, A., Maselli, V., Fulgione, D., et al. (2011). Poly(ADP-Ribose) Polymerase signaling of topoisomerase 1-dependent DNA damage in carcinoma cells. *Biochem. Pharmacol.* 81, 194–202.

References

- Fahrer, J., Popp, O., Malanga, M., et al. (2010). High affinity interaction of poly(ADP-ribose) and the human DEK oncoprotein depends upon chain length. *Biochemistry* 49(33), 7119–7130.
- Feeney, G.P., Errington, R.J., Wiltshire, M., Marquez, N., Chappell, S.C., Smith, P.J. (2003). Tracking the cell cycle origins for escape from topotecan action by breast cancer cells. *Br. J. Cancer* 88(8), 1310–7.
- Ferraris, D.V. (2010). Evolution of Poly(ADP-ribose) Polymerase-1 (PARP-1) Inhibitors. From Concept to Clinic. *J. Med. Chem.* 53(12), 4561-84.
- Gagné, J.P., Isabelle, M., Lo, K.S., et al. (2008). Proteome-wide identification of poly(ADP-ribose) binding proteins and poly(ADP-ribose)-associated protein complexes. *Nucleic Acids Res.* 36(22), 6959-6976.
- Gambi, N., Tramontano, F., Quesada, P. (2008). Poly(ADPR)polymerase inhibition and apoptosis induction in cDDP-treated human carcinoma cell lines. *Biochem. Pharmacol.* 75(12), 2356–63.
- Gilbert, D.C., Chalmers, A.J., El-Khamisy, S.F. (2012). Topoisomerase I inhibition in colorectal cancer: biomarkers and therapeutic targets. *Br. J. Cancer* 106(1), 18-24.
- Haince, J.F., Kozlov, S., Dawson, V.L., Dawson, T.M., Hendzel, M.J., Lavin, M.F., et al. (2007). Ataxia telangiectasia mutated (ATM) signaling network is modulated by a novel poly(ADPribose)-dependent pathway in the early response to DNA-damaging agents. *J. Biol. Chem.* 282, 16441–53.
- Hastak, K., Alli, E., Ford, J.M. (2010). Synergistic chemosensitivity of triple-negative breast cancer cell lines to PARP inhibition, gemcitabine and cisplatin. *Cancer Res.* 70(20), 7970–80.
- Kanai, M., Hanashiro, K., Kim So, H., Hanai, S., Boulares, H.A., Miwa, M., et al. (2007). Inhibition of Crml1–p53 interaction and nuclear export of p53 by poly(ADP-ribosyl)ation. *Nat. Cell. Biol.* 9(10), 1175–83.
- Khanna, K.K., Jackson, S.P. (2001). DNA double-strand breaks: signaling, repair and the cancer connection. *Nat. Genet.* 27, 247-254.
- Krietsch, J., Rouleau, M., Pic, E., et al. (2013). Reprogramming cellular events by poly(ADP-ribose)- binding proteins. *Mol. Aspects Med.* 34(6), 1066-1087.
- Lane, D.L., and Hupp, T.R. (2003). Drug discovery and p53. *D.D.T.* 8, 347–355.
- Madison, D.L., Stauffer, D., Lundblad, J.R. (2011). The PARP inhibitor PJ34 causes a PARP-1- independent, p21 dependent mitotic arrest. *DNA Repair* 10(10), 1003–13.
- Malanga, M., Althaus, F.R. (2004). Poly(ADP-ribose) reactivates stalled DNA topoisomerase I and induces DNA strand break resealing. *J. Biol. Chem.* 279(7), 5244–8.
- Malanga, M., Althaus, F.R. (2005). The role of poly(ADP-ribose) in the DNA damage signaling network. *Biochem. Cell. Biol.* 83(3), 354–64.

References

- Malanga, M., Atorino, L., Tramontano, F., et al. (1998). Poly(ADP-ribose) binding properties of histone H1 variants. *BBA Gene Struct. & Expr.* 1399, 154-160.
- Malanga, M., Pleschke, J.M., Kleczkowska, H.E., Althaus, F.R. (1998). Poly(ADP-ribose) binds to specific domains of p53 and alters its DNA binding functions. *J. Biol. Chem.* 273(19), 11839-43.
- Mashimo, M., Kato, J., Moss, J. (2013). ADP-ribosyl-acceptor hydrolase 3 regulates poly(ADP-ribose) degradation and cell death during oxidative stress. *PNAS U S A* 110(47), 18964-18969.
- Messner, S., Altmeyer, M., Zhao, H., et al. (2010). PARP1 ADP-ribosylates lysine residues of the core histone tails. *Nucleic Acids Res.* 38(19), 6350–6362.
- Nguyen, D., Zajac-Kaye, M., Rubinstein, L., et al. (2011). Poly(ADP-ribose) polymerase inhibition enhances p53-dependent and -independent DNA damage responses induced by DNA damaging agent. *Cell Cycle* 10(23), 4074-82.
- Pommier, Y. (2006). Topoisomerase I inhibitors: camptothecins and beyond. *Nat. Rev. Cancer* 6, 789–802.
- Ray, D., Murphy, K.R., Gal, S. (2012). The DNA binding and accumulation of p53 from breast cancer cell lines and the link with serine 15 phosphorylation. *Cancer Biology & Therapy* 13(10), 848-857.
- Rocco, J.W., Leong, C.O., Kuperwasser, N., DeYoung, M.P., Ellisen, L.W. (2006). p63 mediates survival in squamous cell carcinoma by suppression of p73-dependent apoptosis. *Cancer Cell.* 9(1), 45–56.
- Rolli, V., O' Farrell, M., Ménissier-de Murcia, J., de Murcia, G. (1997). Random mutagenesis of the poly(ADP-ribose) polymerase catalytic domain reveals amino acids involved in polymer branching. *Biochemistry* 36(40), 12147-12154.
- Rouleau, M., Patel, A., Hendzel, M.J., Kaufmann, S.H., Poirier, G.G. (2010). PARP inhibition: PARP1 and beyond. *Nat. Rev. Cancer.* 10, 293–301.
- Sandhu, S.K., Yap, T.A., de Bono, J.S. (2010). Poly(ADP-ribose) polymerase inhibitors in cancer treatment: a clinical perspective. *Eur. J. Cancer* 46(1), 9–20.
- Schavolt, K.L., Pietenpol, J.A. (2007). p53 and Δ Np63 alpha differentially bind and regulate target genes involved in cell cycle arrest, DNA repair and apoptosis. *Oncogene* 26, 6125–32.
- Schreiber, V., Amé, J.C., Dollé, P., Schultz, I., Rinaldi, B., Fraulob, V., Ménissier-de Murcia, J., de Murcia G. (2002). Poly(ADP-ribose) polymerase-2 (PARP-2) is required for efficient base excision DNA repair in association with PARP-1 and XRCC1. *J. Biol. Chem.* 277, 23028-23036.
- Scovassi, A.I., Poirier, G.G. (1999). Poly(ADP-ribosylation) and apoptosis. *Mol. Cell. Biochem.* 199, 125-137.

References

- Smith, L.M., Willmore, E., Austin, C.A., Curtin, N.J. (2005). The novel poly(ADP-Ribose) polymerase inhibitor, AG14361, sensitizes cells to topoisomerase I poisons by increasing the persistence of DNA strand breaks. *Clin. Cancer Res.* 11, 8449–57.
- Tentori, L., Graziani, G. (2005). Chemopotential by PARP inhibitors in cancer therapy. *Pharmacol. Res.* 52, 25–33.
- Tomicic, M.T., Christmann, M., Kaina, B. (2005). Topotecan-triggered degradation of topoisomerase I is p53-dependent and impacts cell survival. *Cancer Res.* 65, 8920-8926.
- Valenzuela, M.T., Guerrero, R., Nunez, M.I., et al. (2002). PARP-1 modifies the effectiveness of p53-mediated DNA damage response. *Oncogene* 21, 1108–1116.
- Wang, M., Wu, W., Wu, W., Rosidi, B., Zhang, L., Wang, H., Iliakis, G. (2006). PARP 1 and Ku compete for repair of DNA double strand breaks by distinct NHEJ pathway. *Nucleic Acids Res.* 34, 6170-6182.
- Wang, Y., Kim, N.S., Haince, J.F., et al. (2011). Poly(ADP-ribose) (PAR) binding to apoptosis-inducing factor is critical for PAR polymerase-1-dependent cell death (parthanatos). *Science Signal.* 4(167).
- Wieler, S., Gagne', J.P., Vaziri, H., Poirier, G.G., Benchimol, S. (2003). Poly(ADP-ribose) Polymerase-1 is a positive regulator of the p53-mediated G1 arrest response following ionizing radiation. *J. Biol. Chem.* 278, 18914–21.
- Yang, A., Kaghad, M., Wang, Y., Gillett, E., Fleming, M.D., Dotsch, V., et al. (1998). p63, a p53 homolog at 3q27–29, encodes multiple products with transactivating, death inducing, and dominant-negative activities. *Mol. Cell.* 2(3), 305–16.
- Yoon, J.H., Ahn, S.G., Lee, B.H., Jung, S.H., Oh, S.H. (2012). Role of autophagy in chemoresistance: regulation of the ATM-mediated DNA-damage signaling pathway through activation of DNA-PKcs and PARP1. *Biochem. Pharmacol.* 83(6), 747–57.



p53 involvement in poly(ADP-ribose) polymerase 1 signaling of topoisomerase I-dependent DNA damage in carcinoma cells

Daniela Montariello, Annaelena Troiano, Maria Malanga, Viola Calabrò, Piera Quesada *

Department of Biology, University of Naples "Federico II", Italy

ARTICLE INFO

Article history:

Received 18 December 2012

Accepted 22 January 2013

Available online 29 January 2013

Keywords:

TOP I inhibitors

PARP1 inhibitors

p53

p63

Carcinoma cells

ABSTRACT

Poly(ADP-ribose)polymerase 1 (PARP-1) inhibitors are thought as breakthrough for cancer treatment in solid tumors such as breast cancer through their effects on PARP's enzymatic activity. Our previous findings showed that the hydrophilic PARP inhibitor PJ34 enhances the sensitivity of p53 proficient MCF7 breast carcinoma cells to topotecan, a DNA Topoisomerase I (TOP 1) inhibitor.

In the present study, we combine the classical TOP 1 poison camptothecin or its water-soluble derivative topotecan with PJ34 to investigate the potentiation of chemotherapeutic efficiency in MCF7 (p53^{WT}), MDA-MB231 (p53^{mut}) breast carcinoma cells and SCC022 (p53^{null}) squamous carcinoma cells.

We show that, following TPT-PJ34 combined treatment, MCF7 cells exhibit apoptotic death while MDA-MB231 and SCC022 cells are more resistant to these agents. Specifically, in MCF7, (i) PJ34 in combination with TPT causes a G2/M cell cycle arrest followed by massive apoptosis; (ii) PJ34 addition reverts TPT-dependent PARP-1 automodification and triggers caspase-dependent PARP-1 proteolysis; (iii) TPT, used as a single agent, stimulates p53 expression while in combination with PJ34 increases p53, TAp63 α and TAp63 γ protein levels with a concomitant reduction of MDM2 protein.

The identification of p63 proteins as new players involved in the cancer cell response to TPT-PJ34 is relevant for a better understanding of the PARP1-dependent signaling of DNA damage. Furthermore, our data indicate that, in response to TPT-PJ34 combined chemotherapy, a functional cooperation between p53 and TAp63 proteins may occur and be essential to trigger apoptotic cell death.

© 2013 Elsevier Inc. All rights reserved.

1. Introduction

Poly(ADP-ribose)polymerase (PARP) inhibitors are touted as a breakthrough for cancer treatment in solid tumors such as triple negative breast cancer and ovarian cancer through their effects on PARP-1's enzymatic ADP ribosylation activity [1]; however, less characterized PARP-1 additional functions have also been reported and they can be critical for successful anticancer therapies.

PARPs are involved in the regulation of many cellular processes such as DNA repair, cell cycle progression and cell death [2]. PARP-1 and PARP-2 are constitutive factors of the DNA damage surveillance network, acting as DNA break sensor [3] and several observations indicate that poly(ADP-ribosyl)ation plays an early role in DSB signaling and repair pathways [4,5]. PARP-1 and 2 are highly activated upon binding to DNA strand interruptions and synthesize, within few seconds, large amounts of ADP-ribose polymer (PAR) on several nuclear proteins including themselves, histones, DNA-Topoisomerase 1 (TOP 1) and DNA-dependent

protein kinase (DNA-PK) [6,7]. Furthermore, in response to DNA damage, PARP-1 interacts with both ATR and ATM kinases suggesting another susceptible pathway for PARP inhibitors induced apoptosis. [8].

Cell cycle checkpoint activation and growth arrest in response to DNA damage rely on the ATM/ATR kinases and their downstream targets like p53 [9–11]. p53 activates p21WAF which binds PARP-1 during base excision repair [12].

Certain PARP inhibitors including PJ34 induce a G2/M arrest when used in conjunction with methylating agents [13] cisplatin [14] and TOP I poisons such as camptothecin (CPT) or its water-soluble derivative topotecan (TPT) [15], highlighting the existence of potentially different outcomes from PARP inhibition whose molecular mechanisms have not yet been conclusively determined.

In brief, TOP I inhibitors reversibly abolish the DNA religation activity of TOP I generating single strand breaks (SSBs) to which the protein is covalently linked. Double strand breaks (DSBs) arise when replication forks collide with the SSBs and run off. Thus, CPT/TPT-induced DSBs are replication dependent or S phase specific and are usually repaired by the HR pathway [16,17]. According with previous findings poly(ADP-ribosyl)ated PARP-1 and PARP-2 counteract CPT through non covalent but

* Corresponding author. Tel.: +39 081 679165; fax: +39 081 679233.

E-mail address: quesada@unina.it (P. Quesada).

specific interaction of PAR with some TOP I sites which results in inhibition of DNA cleavage and stimulation of the religation reaction [6].

We have previously shown that PJ34 can positively or negatively modulate p53 and its target p21WAF depending of the cell genetic background or DNA damage stimulus (i.e. cisplatin or TPT) [18–20]. Indeed, regulating p21WAF expression is one model whereby PARP inhibitors, following the activation of different checkpoint pathways, can cause cell cycle arrest. It has recently been reported that in breast carcinoma MCF7 cells, PJ34 causes a p21WAF-dependent mitotic arrest and that neither PARP-1 nor p53 is required for this mechanism [21]. Furthermore, in triple negative breast cancer cell lines, PJ34 synergizes with cisplatin by reducing the levels of Δ Np63 α with a concurrent increase of p21WAF [22].

Δ Np63 α is a member of the p53 protein family highly expressed in squamous cell carcinoma and invasive ductal breast carcinoma [23,24]. Δ Np63 α and p53 have been shown to inversely regulate target genes such as p21WAF in the context of DNA damage [22,25]. Owing to the presence of two promoters, the p63 gene encodes two major classes of proteins: those containing a transactivating (TA) domain homologous to the one present in p53 (i.e. TAp63) and those lacking it (i.e. Δ Np63) [24]. In addition, alternate splicing at the carboxy-terminal (C-terminal) generates at least three p63 variants (α , β and γ) in each class. The TAp63 γ isoform resembles most p53, whereas the α isoforms include a conserved protein–protein interaction domain named Sterile Alpha Motif (SAM). TAp63 proteins mimic p53 function including transactivating many p53 target genes and inducing apoptosis, whereas the Δ Np63 α protein, has been shown to repress p53-target genes acting as an oncogene [24,26].

On the light of all these evidences, the use of chemical inhibitors of PARP in combination with TOP I inhibitors CPT or TPT appears to be a promising approach to enhance the antitumour activity of these compounds.

Here, we have investigated the effect of PJ34 used as a single agent or in association with CPT or TPT in the DNA damage response of mammary breast cancer cells (MCF7^{p53wt} and MDA-MB231^{p53mut}) and squamous carcinoma cells (SCC022^{p53null}) showing an active involvement of p63 in the cellular response to these agents. We postulate that the sensitivity to combined treatments is mediated by sustained DNA damage/inefficient DNA repair triggering p53 and p63-mediated apoptosis.

2. Materials and methods

2.1. Drugs, media, antibodies and chemicals

CPT and TPT was from Glaxo Smith-Kline (Verona, Italy) and PJ34 [N-(6-oxo-5,6-dihydrophenanthridin-2-yl)-(N,N-dimethylamino) Acetamide] from Alexis Biochemicals (Vinci-Biochem, Firenze, Italy). The cocktail of protease inhibitors was from ROCHE-Diagnostic (Milano, Italy).

MCF7, MDA-MB231 and SCC022 cells were from CLS Cell Lines Service (Eppelheim, Germany) Dulbecco's modified Eagle's medium (DMEM), heat-inactivated foetal bovine serum (FBS) and Roswell Park Memorial Institute (RPMI) medium were from Invitrogen (GIBCO, Milano, Italy); penicillin, streptomycin and L-glutamine were from LONZA (Milano, Italy).

Nicotinamide adenine [adenylate-³²P] dinucleotide-[³²P]-NAD⁺ (1000 Ci/mmol, 10 mCi/ml) was supplied by GE Healthcare (Milano, Italy).

PVDF (poly-vinylidene-fluoride) membrane was from MILLIPORE S.p.A. (Milano, Italy). Not-fat-milk powder was from EUROCLONE (Milano, Italy). Anti-DNA TOP I (ScI-70) human antibody from Topogen (ABCAM, Cambridge, UK). Anti-PARP1 mouse

monoclonal antibody (C2-10), anti-p63 (4A4), anti-p53 (DO-1), anti-p21WAF (F-5), anti-cyclin B1 (V152), anti-AIF (E-1) and anti-GAPDH (6C5) mouse monoclonal antibodies and anti-actin (H-196) rabbit polyclonal antibody were from Santa-Cruz Biotechnology (DBA, Milano, Italy). Anti- γ H2AX (ser139, 2577) and anti-Bax (D2E11) rabbit polyclonal antibodies were from Cell Signaling (Invitrogen, Milano, Italy). Anti-MDM2 (Ab-2) mouse monoclonal antibody was from Oncogene Research Products (Boston, USA). Anti-PAR (10H) mouse monoclonal antibody was from Alexis Biochemicals (Vinci-Biochem, Firenze, Italy). Goat anti-mouse and goat anti-rabbit IgG HRP-conjugated antibodies were from Sigma-Aldrich (Milano, Italy).

All other chemicals analytical grade were of the highest quality commercially available.

2.2. Cell cultures

Breast cancer-derived MCF7^{p53wt} and MDA-MB231^{p53mut} cells were maintained in Dulbecco's modified Eagle's medium (DMEM) containing 10% (v/v) heat-inactivated foetal bovine serum (FBS), while squamous SCC022^{p53 null} carcinoma cells were maintained in Roswell Park Memorial Institute (RPMI) medium containing 10% (v/v) FBS, 100 U/ml penicillin, 100 g/ml streptomycin, 5 mM L-glutamine and incubated at 37 °C in a humidified atmosphere, plus 5% CO₂.

2.3. Cell treatments

Cells were seeded at 1×10^6 cells in 10 ml and 24 h after seeding, treated with 1 μ M CPT (stock solution 1 mM DMSO) or 5 μ M TPT, 10 \times concentration inhibiting cellular growth by 50% (IC₅₀) [27]. 10 μ M or 20 μ M PJ34 alone and in combination, for 48 h in fresh medium. Culture medium was removed and, after PBS wash, cells were recovered 6×10^6 cells/ml in 50 mM Tris-HCl pH 7.5, 150 mM NaCl, 5 mM EDTA, 1% NP40 (Lysis Buffer) plus 2 mM PMSF and 1:25 dilution of protease inhibitors cocktail solution. After 40 min of incubation on ice, cellular suspensions were scraped and centrifuged at $16,000 \times g$ for 20 min at 4 °C.

Cell growth inhibition was assessed by cell counting at different time points (0–24 h) or by the 3-[4,5-dimethylthiazol-2-yl]-2,5-diphenyltetrazolium bromide (MTT) assay using 1×10^4 48 h treated cells. The experiments were performed in triplicate.

2.4. Isolation of nuclear and post-nuclear fractions

To isolate sub-cellular fractions, 3×10^6 cells were suspended in 200 μ l of 30 mM Tris-HCl pH 7.5 buffer, containing, 1.5 mM MgCl₂, 10 mM KCl, 1% (v/v) Triton X-100, 20% glycerol, 2 mM PMSF and 1:25 dilution of protease inhibitors cocktail solution. After 30 min of incubation on ice, cellular suspensions were centrifuged at $960 \times g$ for 90 s at 4 °C and the nuclear fractions recovered in the pellet. The supernatant represents the cytoplasmic fraction.

Nuclear fractions were resuspended in 50 μ l of 20 mM HEPES pH 7.9 buffer, containing 20 mM KCl, 0.2 mM EDTA, 1.5 mM MgCl₂, 25% glycerol and the protease inhibitors cocktail solution. Protein concentration was determined using the Bradford protein assay reagent (BIO-RAD Milano, Italy) with bovine serum albumin as a standard.

2.5. Cytofluorimetric analysis

Control and treated cells were fixed in 70% ethanol and stored at –20 °C until analysis. After a washing in PBS w/o Ca²⁺/Mg²⁺, cells were stained in 2 ml of propidium iodide (PI) staining solution [50 μ g/ml of PI, 1 mg/ml of RNase A in PBS w/o Ca²⁺/Mg²⁺, pH 7.4] overnight at 4 °C and DNA flow cytometry was performed in

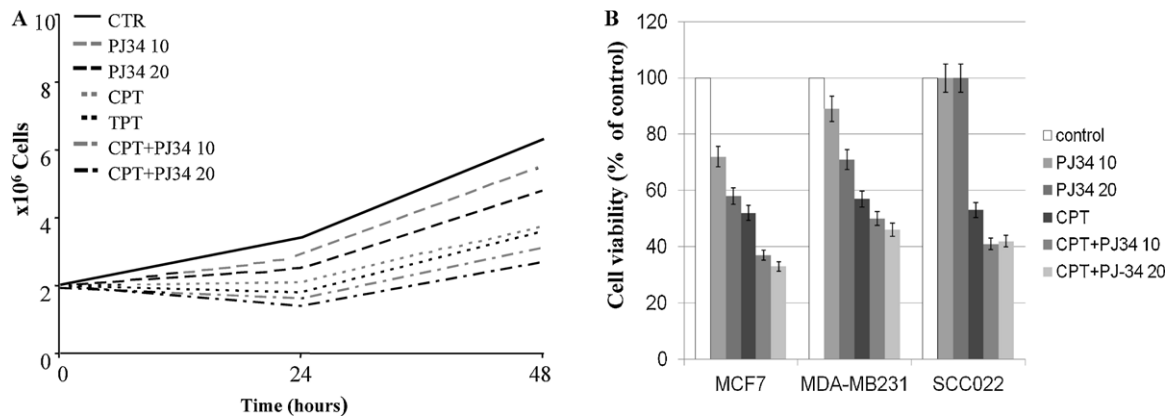


Fig. 1. Cell growth inhibition in MCF7, MDA-MB231 and SCC022 cells treated with CPT/TPT and PJ34 as single agents or in combination. Cells (10^4 cells/plate) were treated 48 h with CPT 1 μ M or TPT 5 μ M and 10 or 20 μ M PJ34 alone or in combination: (A) MCF7 cell growth was measured by cell counting at different time points. Data refer to at least three experiments giving similar results. (B) 48 h treated MCF7, MDA-MB231 and SCC022 cells were used for determination of cell growth inhibition by MTT assay. Each plot represents the media of triplicates from three independent experiments.

duplicate by a FACScan flow cytometer (Becton Dickinson Franklin Lakes, NJ, USA) coupled with a CICERO work station (Cytomation). Cell cycle analysis was performed by the ModFit LT software (Verity Software House Inc., Topsham, ME, USA). FL2 area versus FL2 width gating was done to exclude doublets from the G2/M region. For each sample 15,000 events were stored in list mode file.

2.6. Analysis of [32 P]-PAR synthesis

Following treatment with CPT/TPT \pm PJ34 of intact cell (5×10^4 cells/plate), [32 P]-PAR synthesis was determined by substituting the culture medium with 1 ml of 50 mM HEPES pH 7.5 buffer, containing 28 mM KCl, 28 mM NaCl, 2 mM MgCl₂, 0.01% digitonin, 0.1 mM PMSF, 1:25 dilution of a cocktail of protease inhibitors, 0.125 μ M NAD⁺ and 5 μ Ci [32 P]-NAD⁺ (1000 Ci/mmol). After incubation at 37 °C for 15 mins, cells were scraped, transferred to eppendorf tubes and mixed with TCA at 20% (w:v) final concentration. After 90 min standing on ice, samples were collected by centrifugation at 12000 rpm for 15 min, washed twice with 5% TCA and three times with ethanol. [32 P]-PAR incorporated in the TCA-insoluble fraction was measured by Cerenkov counting using a LS8100 liquid scintillation spectrometer (Beckman Coulter S.p.A. Milano, Italy). Finally, TCA protein pellets were resuspended in Laemmli buffer; proteins were separated by 10% SDS-PAGE and after electroblotting on PVDF membrane, [32 P]-PAR acceptors were visualized by autoradiographic analysis by the PhosphorImager (BIO-RAD). Immunodetection of specific proteins was accomplished on the same blots after autoradiography.

2.7. Immunological analyses

Aliquots of 10 μ l of cellular proteins (approx 50–100 μ g) were separated by 10% SDS-PAGE and transferred onto a PVDF membrane using an electroblotting apparatus (BIO-RAD). The membrane was subjected to immunodetection after blocking with 5% non-fat milk in TBST 1 h, with anti-PARP1 (C2-10; diluted 1:2500), anti-TOP I (Sc1-70; diluted 1:1000), anti-PAR (10H; diluted 1:500), anti-p63 (4A4; diluted 1:2000), anti-p53 (DO-1; diluted 1:5000), anti-p21WAF (F-5; diluted 1:1000), anti-MDM2 (Ab-2; diluted 1:1000), anti-cyclin B1 (V152; diluted 1:1000), anti- γ H2AX (2577; diluted 1:1000), anti-Bax (D2E11; diluted 1:1000), anti AIF (E1; diluted 1:2000), anti-GAPDH (6C5; diluted 1:5000), anti-actin (H-196; diluted 1:2000) overnight at room temperature.

As secondary antibodies goat-anti-mouse or goat-anti-rabbit IgG HRP-conjugate (diluted 1:5000–1:10,000) in 3% (w/v) non-fat

milk in TBST were used. Peroxidase activity was detected using the ECL Advance Western Blot Kit of GE Healthcare (Milano, Italy) and quantified using the Immuno-Star Chemiluminescent detection system GS710 (BIO-RAD) and the Arbitrary Densitometric Units normalised on those of the GAPDH loading control.

3. Results

3.1. Effect of PJ34 on TPT/CPT-induced growth inhibition in human carcinoma cells

The concentrations of the agents and the time points used in this study were chosen on the basis of previously published data [20,27]. Preliminary experiments, in breast carcinoma MCF7^{p53wt} cells, showed that 1 μ M CPT inhibits cell growth similarly to 5 μ M TPT (Fig. 1A). To potentiate the CPT/TPT cytostatic effect, PJ34 concentrations were used in a sub-lethal range (10–20 μ M). A 48-h of exposure, corresponding approximately to two rounds of MCF7^{p53wt} cell replication, was used according to the administration procedure during anticancer therapy. As shown in Fig. 1A, at 24 h CPT/TPT treatment has a cytostatic effect, while PJ34 induces growth retardation in a dose-dependent way, whereupon cells start to recover but the rate of recovery was significantly affected by CPT-PJ34 combined treatment (Fig. 1A).

We next investigated the impact of CPT on MDA-MB231 and SCC022 cell survival. MDA-MB231 express a mutant p53 (p53R280K) while SCC022 cells are p53 null. Cells were plated, treated with CPT for 48 h and subjected to the MTT assay to compare viability of treated and untreated cells. As shown in Fig. 1B, CPT significantly reduces cell viability of all cell lines tested (around 50% of control). Moreover, treatment with PJ34 alone affects MCF7 and MDA-MB231 cell viability, in a dose-dependent way, whereas SCC022 cells remain almost unaffected. Interestingly, compared with single drug treatments, combination of PJ34 with CPT results in a significant enhancement of cytotoxicity in MCF7 cells (37–33% of cell survival) while in MDA-MB231 and SCC022 cells addition of PJ34 to CPT has a lower impact on cell survival (Fig. 1B). Similar results are observed when PJ34 is added to TPT (data not shown).

We have previously reported that TPT at concentrations higher than 1 μ M promptly arrested the cells in S phase while concentrations equal or lower than 1 μ M cause a G2/M arrest [20]. To gain insight into the molecular mechanism of TPT-PJ34 interactive cytotoxicity we analysed the cell cycle distribution of MCF7 cells treated with 10 or 20 μ M PJ34 alone or in combination with 1 μ M TPT. As shown in Fig. 2, after 48 h treatment, 1 μ M TPT

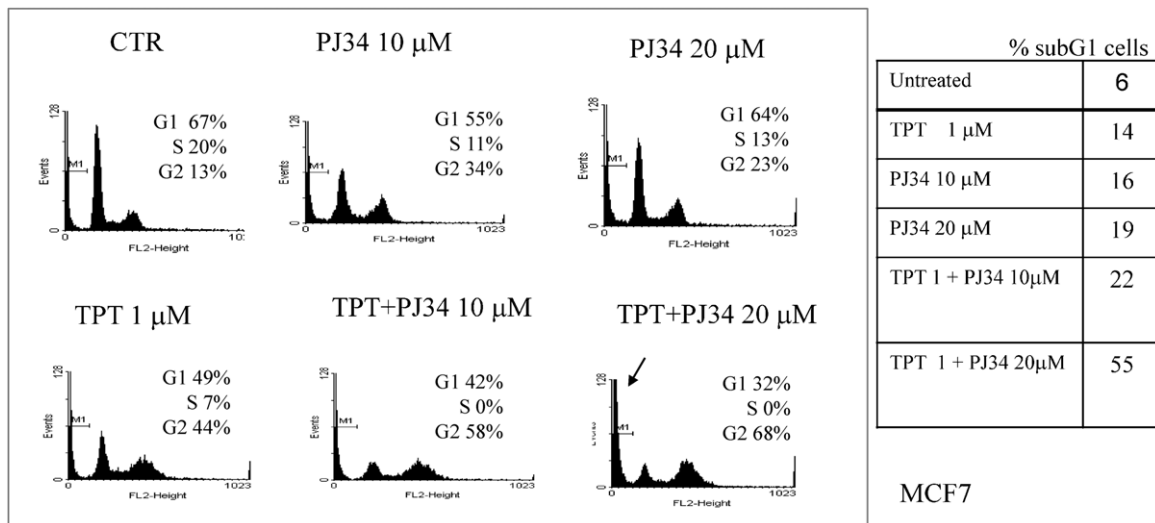


Fig. 2. Cell cycle analysis of MCF7 cells subjected to TPT and PJ34 single and combined treatments. MCF7 cells were treated 48 h with TPT 1 μM and 10 or 20 μM PJ34 alone or in combination. Control and treated cells (1×10^6) were fixed in 70% ethanol and used for flow cytometric analysis (see Section 2). Determination of DNA content after PI staining is shown and cells in G1, S and G2 phase are indicated as percentage (excluded sub-G1 cells). The table reports sub-G1 cells as the percentage of the entire population of cells. Data refer to one of three experiments giving similar results.

as well as 10 or 20 μM PJ34 induce accumulation of cells in G2/M phase and the cell cycle distribution is less affected by treatment with PJ34 (10 or 20 μM) than TPT used as single agents. Furthermore, addition of 10 or 20 μM PJ34 to 1 μM TPT causes a significant increase of G2/M cells, while S-phase cells are drastically reduced. Fig. 2 (table) also shows that single treatments cause an increase of cells with a sub-G1 DNA content (from 6 to 19%), probably due to induction of apoptotic cell death. Remarkably, an increase up to 55% of sub-G1 cells is observed with TPT 1 μM + PJ34 20 μM combined treatment, showing a 2× potentiation factor of PJ34 on TPT cytotoxicity.

3.2. Analysis of CPT- or TPT-dependent TOP I inactivation

It is already known that CPT and TPT abolish the religation activity of TOP I generating an abortive complex to which the enzyme is covalently linked [16]. Therefore, we determined the efficacy of TOP I inhibitors by looking at their capacity of trapping the enzyme in the abortive complex. This was detected, by looking at the disappearance of the immunoreactive band of the TOP I soluble fraction by western blot analysis. After 48 h of treatment, both 1 μM CPT and 5 μM TPT are able to block, almost completely, the TOP I enzyme in the abortive complex, in all cell lines tested (Fig. 3).

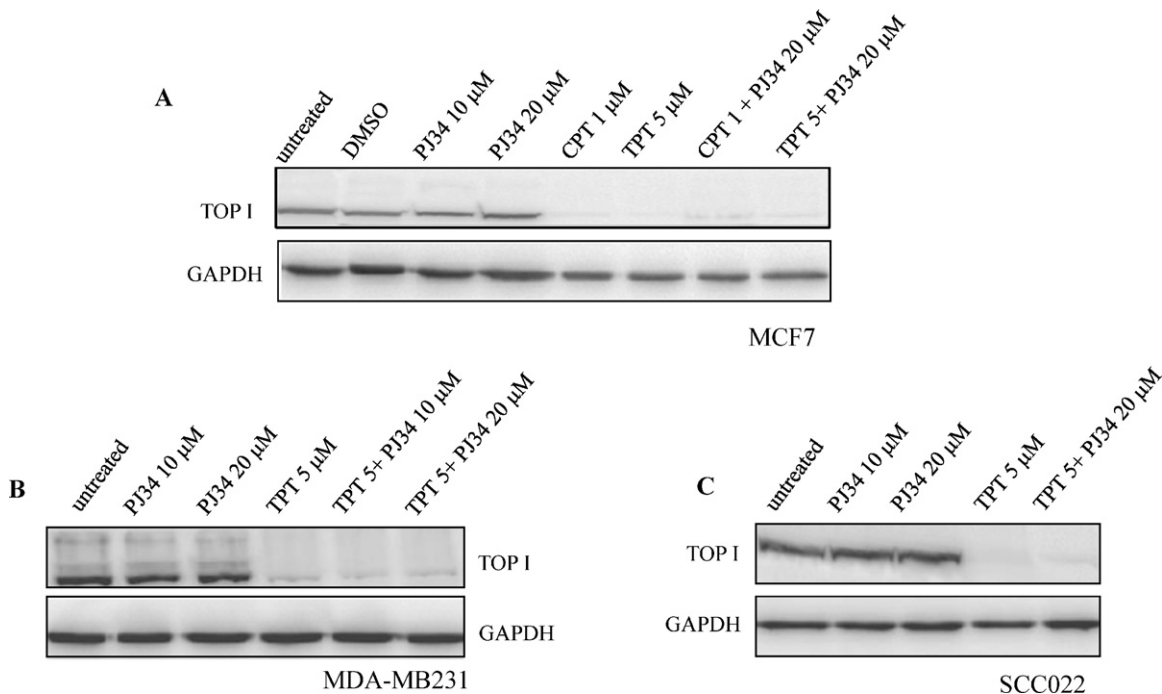


Fig. 3. Western blot analysis of TOP I soluble fraction in carcinoma cells untreated or 48 h treated with the indicated drugs. Untreated and treated whole cell extracts (50–100 μg of proteins) were subjected to 10% SDS-PAGE, electroblotted on PVDF and incubated with the anti-TOP I antibody. Immunodetection in MCF7 (A), MDA-MB231 (B) and SCC022 (C) cells is shown. 0.1% DMSO treated cells were analysed as CPT internal control. GAPDH was used as loading control.

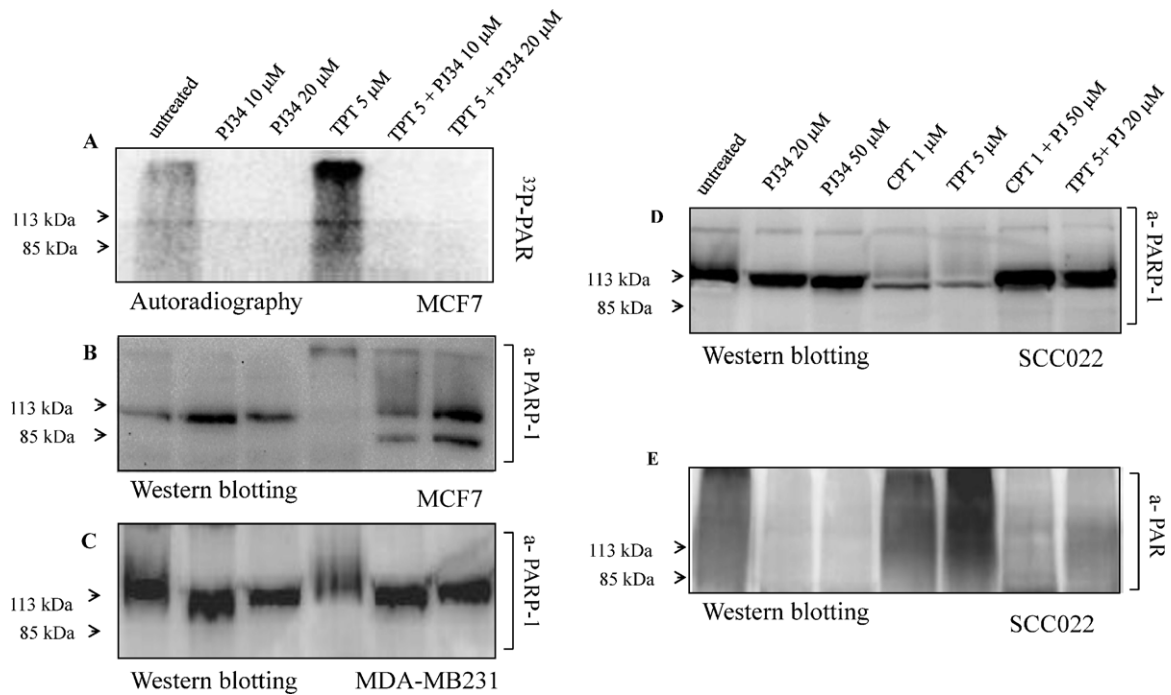


Fig. 4. Analysis of TPT-dependent PARP-1 activation or PJ34-dependent PARP-1 inhibition in carcinoma cells untreated or 48 h treated with the indicated drugs. Whole cell extract (50–100 μg of proteins) after 10% SDS-PAGE and electroblotting on PVDF were either analysed by autoradiography or incubated with the different antibodies. (A) Autoradiographic analysis, of whole cell protein extract from untreated and treated MCF7 cells incubated with $0.125 \mu\text{M}$ [^{32}P]-NAD $^+$ (see Section 2); (B) immunodetection of PARP-1 on the blot shown in (A); (C) immunodetection of PARP-1 in whole cell protein extract from untreated and treated MDA-MB231 cells; (D) immunodetection of PARP-1 in whole cell protein extract from untreated and treated SCC022 cells; (E) immunodetection of PAR on the blot shown in (D)

According to previous findings [20], PJ34 does not affect TOP I enzyme trapping when used in combination with CPT or TPT.

3.3. Analysis of PAR synthesis in carcinoma cells after treatment with TPT \pm PJ34

PJ34 efficacy as PARP inhibitor was assessed by looking at its effect on PARP-1 automodification. Proliferating MCF7 cells were exposed to the drugs and PAR synthesis was measured *in situ* by incubation in the presence of 0.01% digitonin with $0.125 \mu\text{M}$ [^{32}P]-NAD $^+$. Samples were then analysed by SDS-PAGE followed by autoradiography. As shown in Fig. 4A, a smear of the signal above the PARP-1 molecular weight (113 kDa) is strongly increased in TPT treated cells compared to the untreated sample (Fig. 4A, lane 4). As previously reported [2] such a behaviour indicates automodification of PARP-1 by long and branched ADP-ribose polymers (up to 200 residues in chain) on several sites (up to 25) of the automodification domain. This process gives rise to higher molecular weight PARP-1 forms that do not enter the polyacrylamide gel matrix. The identity of the PAR modified protein was confirmed by western blotting using a PARP-1 antibody showing a mobility shift of the immunoreactive band at the top of the gel (Fig. 4B, lane 4). According to our observation, the autoradiographic signals are absent in cells treated with the PARP-1 inhibitor alone (Fig. 4A, lanes 2 and 3) or in combination with TPT (Fig. 4A, lanes 5 and 6). Interestingly, TPT–PJ34 co-treatment in MCF7 cells induced apoptosis as demonstrated by the appearance of the 85 kDa fragment generated by the caspase-dependent cleavage of PARP-1 (Fig. 4B, lanes 5 and 6).

Immunoblot analysis with PARP-1 antibody was also performed in MDA-MB231 cells subjected to the same treatments. As shown in Fig. 4C, in TPT-treated cells PARP-1 is automodified to a lower extent (lane 4) and there are no signs of apoptosis induction after TPT–PJ34 combined treatment (Fig. 4C, lanes 5 and 6).

Furthermore, we analysed the response of SCC022 squamous carcinoma cells to PJ34 and TPT treatment. Immunoblot with the PARP-1 specific antibody reveals that PARP-1 is modified since the unmodified 113 kDa band is strongly reduced (Fig. 4D, lanes 4 and 5). Accordingly, immunoblot using a PAR antibody shows a smeared signal of long and branched polymers above the PARP-1 molecular weight (Fig. 4E, lanes 4 and 5). PJ34 co-treatment drastically reduces TPT/CPT-induced PARP-1 automodification thus leading to the accumulation of the 113 kDa band of PARP-1. However, we did not observe PARP-1 specific cleavage, thereby suggesting that cells were not undergoing apoptosis albeit up to $50 \mu\text{M}$ PJ34 was used (Fig. 4D, lanes 6 and 7). All together, our results suggest that, compared to MCF7, MDA-MB231 and SCC022 cells are less sensitive to the drugs combination and do not respond immediately with apoptosis to TOP I and PARP-1 inhibitors co-treatment.

3.4. Involvement of p63 in the cell response to TPT \pm PJ34 treatment

To get insight into the molecular mechanism underlying the response of MCF7 cells to TPT \pm PJ34 treatment, we analysed the expression of p53, p63 and other cell cycle markers such as p21WAF, MDM2 and cyclin B1. In MCF7 cells we found that PJ34 addition to TPT strongly enhances the TPT-dependent stimulation of p53 expression. Remarkably, the p53 negative regulator MDM2 was down-regulated only upon combined treatment (Fig. 5A). Furthermore, using the 4A4 monoclonal antibody which recognizes all p63 isoforms, we only detected bands corresponding to the pro-apoptotic TAp63 α and γ isoforms; both isoforms are up-regulated by TPT–PJ34 co-treatments (Fig. 5A). Quantitation of proteins by densitometric scanning, reveals a 19–20-fold increase of the expression level for both p53 and p63 proteins after TPT–PJ34 $20 \mu\text{M}$ treatment (Fig. 5B). The increase of p21WAF expression level was concomitant to a decrease of cyclin B1 thereby supporting the G2/M cell cycle arrest observed by cytofluorimetric analyses.

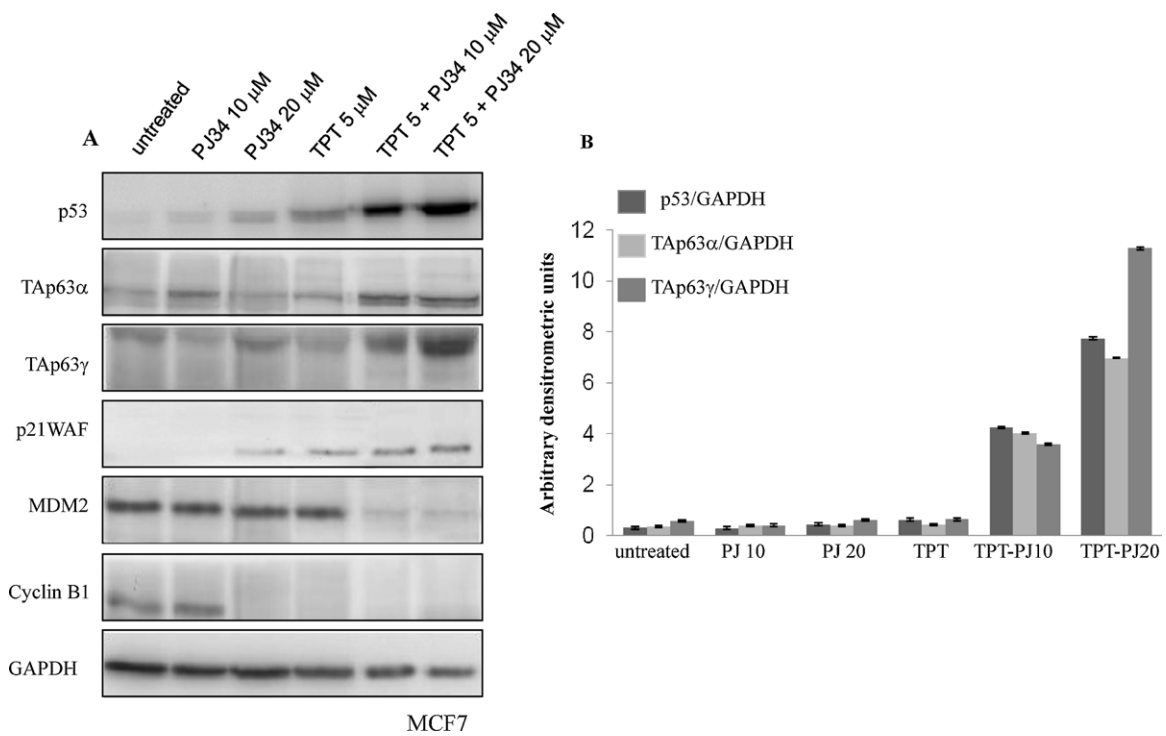


Fig. 5. Western blot analysis of p53, p63, p21WAF, MDM2 and cyclin B1 expression in MCF7 cells untreated or 48 h treated with the indicated drugs. Whole cell extract (50–100 μ g of proteins) after 10% SDS-PAGE and electroblotting on PVDF were incubated with the different antibodies. (A) Immunodetection of p53, p63, p21WAF, MDM2, cyclin B1. GAPDH was used as loading control; (B) p53 and TAp63 α and γ band intensities were quantified by densitometric scanning. Data expressed as Arbitrary Densitometric Units (ADU) were normalized to the internal control GAPDH. Shown are the mean of three different experiments \pm S.E.

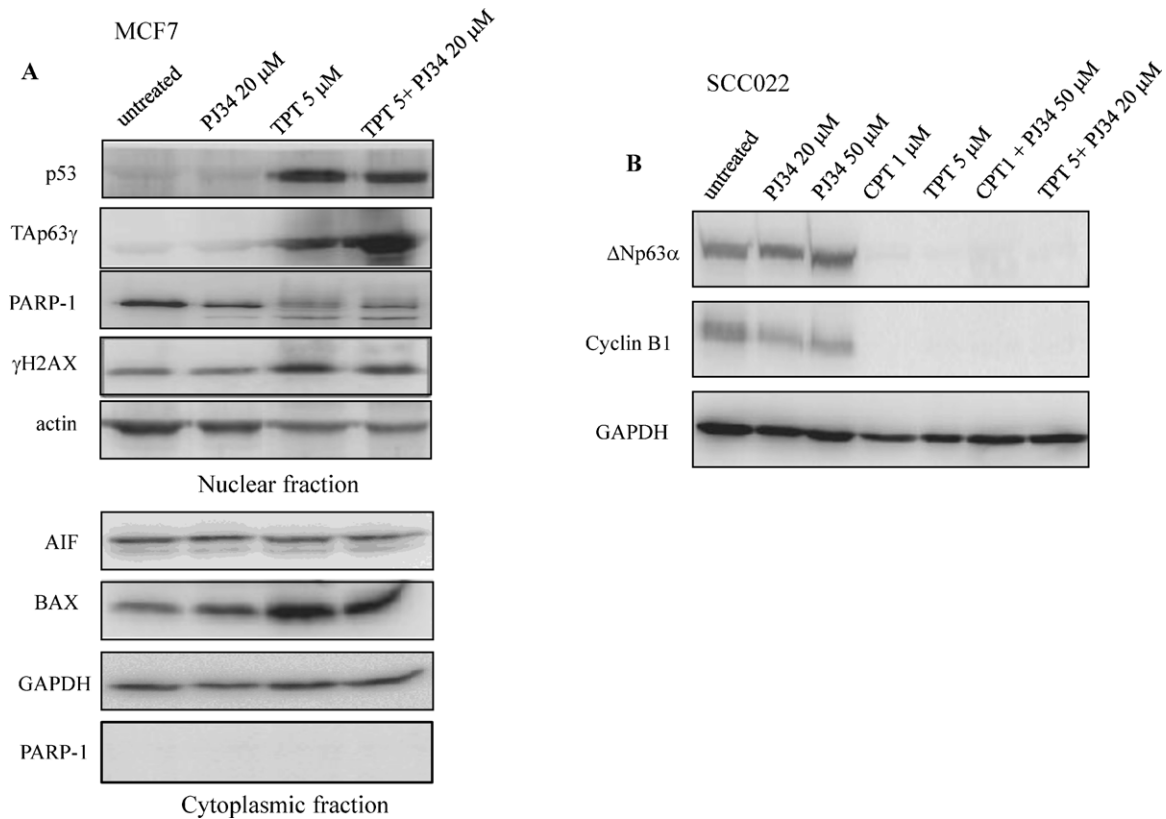


Fig. 6. Western blot analysis of protein extract from nuclear and cytoplasmic fraction of MCF7 cells and from SCC02 cells untreated or 48 h treated with the indicated drugs. Whole extract (50–100 μ g of proteins) after SDS-PAGE and electroblotting on PVDF were incubated with the different antibodies. (A) Immunodetection of p53, p63, PARP-1, γ H2AX, BAX, AIF in nuclear (upper panel) and cytoplasmic (lower panel) fractions from MCF7 cells. Actin and GAPDH were used as loading controls, respectively; (B) immunodetection of p63 and cyclin B1 in SCC022 cell extract. GAPDH was used as loading control.

We also performed immunoblot analysis of MCF7 nuclear and cytoplasmic fractions. Fig. 6A shows that following TPT ± PJ34 treatment both p53 and Tap63 γ accumulate in the nuclear compartment. Nuclear γ H2AX expression and PARP-1 specific cleavage were monitored as markers of dsDNA damage and caspase-dependent apoptosis, respectively (Fig. 6A, upper panel). Furthermore, the expression level of the pro-apoptotic BAX protein, whose gene is transcriptionally activated by p53 and Tap63, increases in the cytoplasmic fraction by either TPT alone or TPT–PJ34 combined treatment, while the level of the mitochondrial apoptosis inducing factor AIF is unaffected (Fig. 6A, lower panel).

Finally, as shown in Fig. 6B, in p53 null SCC022 cells, the Δ Np63 α anti-apoptotic isoform is dramatically down-regulated by CPT/TPT treatment with or without PJ34. Cyclin B1 appears to be concomitantly reduced suggesting a G2/M cell cycle arrest. Importantly, using the 4A4 antibody, we were unable to detect p63 isoforms other than Δ Np63 α both in untreated and TPT ± PJ34 treated SCC022 cells (data not shown). It has previously been demonstrated that Δ Np63 α is required for the survival of SCC cells [27]. Interestingly, as shown in Fig. 4D, CPT/TPT ± PJ34 treatments was not sufficient to induce apoptosis in these cells thereby suggesting the existence of an alternative anti-apoptotic pathway able to overcome Δ Np63 α depletion. In MDA-MB231 cells, no p63 immunoreactive bands were seen in all experimental conditions (data not shown) thereby excluding a possible role for p63 in TPT ± PJ34-induced cytotoxicity in this cellular context.

4. Discussion

The efficacy of PARP inhibitors as chemosensitizers has led to the development of a multitude of such molecules with different bioavailability and pharmacokinetic properties that are currently under investigation in clinical trials [1]. However, a clear understanding of how PARP inhibitors potentiate the activity of antineoplastic agents is still lacking.

The hydrophilic PARP inhibitor PJ34 has already been reported to synergize with cisplatin- and TPT-dependent apoptotic induction in triple-negative breast cancer and human carcinoma cells expressing wild type p53 [19–22]. We have already shown that PJ34, at a concentration of 5 μ M, inhibits PARP-1 activity without cytotoxic effects. Furthermore, in HeLa and MCF7 cells we found that TPT toxicity was higher when PAR synthesis was reduced by either PARP-1 silencing or PJ34 administration [20].

In the present study, we compared the response of MCF7^{p53wt}, MDA-MB231^{p53mut} and SCC022^{p53null} cells to treatment with higher concentration of PJ34 (up to 20 μ M) in combination with 1 μ M CPT or 5 μ M TPT. According to the previously reported specificity of PARP inhibitors for breast cancer [1,29], we observed a higher sensitivity to PJ34 in MCF7^{p53wt} cells. In such cells we confirmed that TPT, which is known to be S-phase specific [30], causes a G2/M cell cycle arrest when used at a lower concentration (1 μ M). In addition, the TPT-dependent G2/M cell cycle arrest was enhanced by TPT + PJ34 combined treatment and resulted in a remarkable increase of cells with sub-diploid DNA, confirming a synergic cytotoxic effect of TOP I and PARP-1 inhibitors.

Consistent with the idea that poly(ADP-ribosylation) plays a role in the response to CPT/TPT-induced DNA damage we observed the disappearance of a TOP I soluble/active fraction and the PARP-1 automodification in MCF7, MB-MDA231 and SCC022 cells thereby indicating that the response to DNA damage, induced by TOP I inhibitors, in skin squamous carcinoma cells is similar to that observed in breast carcinoma cells [31].

On the other hand, we found that prevention of PARP-1 automodification by PJ34 induces PARP-1 proteolysis only in MCF7^{p53wt} implying that apoptosis induced by inhibition of PAR synthesis requires the p53 wild type activity. Given the similarity

between p53 and p63 it was of interest to look at the effect of TOP I + PARP-1 inhibitors on p63 protein isoforms. Interestingly, TPT + PJ34 treatment in MCF7 cells causes a remarkable increase of Tap63 α and γ protein levels. Tap63 γ in particular, was reported to be a potent apoptosis inducer [32]. Both p53 and Tap63 γ accumulated in the nuclear fraction where the proteins can functionally interact in the control of transcription. Consistently, TPT + PJ34 combined treatment caused a dramatic reduction of MDM2, a negative regulator of p53 transcriptional activity and protein level.

Remarkably, this is the first evidence of a PJ34-inducible pro-apoptotic response involving both p53 and p63 family members in breast carcinoma cells. Furthermore, in SCC022^{p53null} cells we show that CPT/TPT single or combined treatments suppressed the endogenously expressed Δ Np63 α anti-apoptotic isoform together with cyclin B1. It has previously been demonstrated that Δ Np63 α is required for the survival of SCC cells by virtue of its ability to suppress p73-dependent apoptosis [28]. However, CPT/TPT ± PJ34 treatments is not sufficient to induce apoptosis in these cells thereby suggesting either the presence of a non-functional p73 or the existence of an alternative anti-apoptotic pathway able to overcome Δ Np63 α depletion. Similarly, it has been reported that in MDA-MB468 cells expressing high level of Δ Np63 α , PJ34 reduced Δ Np63 α level, with a concomitant increase of p73. However, in that manuscript, apoptosis induction was not evaluated [22].

Therefore, it can be postulated that carcinoma cells, depending on their genetic background (p53/p63 null versus p53/p63 proficient), can trigger a p53-dependent pathway to induce cell cycle arrest and apoptosis, as a results of concomitant inhibition of PARP-1 and TOP I. To this respect, the particular p63 isoform expressed may sustain (Tap63 α and γ) or inhibit (Δ Np63 α) the execution of the apoptotic program.

Recently, it has been shown that PARP activity is required for TOP I poisoning-mediated replication fork slowing [33] and reversal [34]. In fact, PARP-1 is able to slow replication fork progression in response to CPT-dependent HR DNA repair. Furthermore, these data identify fork reversal as a means to prevent chromosome breakage upon exogenous replication stress and implicate still undefined proteins involved in fork reversal or restart as factors modulating the cytotoxicity of replication stress-inducing chemotherapeutics.

We have identified p63 as a new player of the PARP1-dependent signalling of DNA damage. Interestingly, in the p63 DNA binding domain, both the PAR binding motif and the glutamic acid residues showed to act as covalent PAR acceptor sites are conserved [35,36]. Our findings contribute to the understanding of the molecular events triggered by TOP I and PARP-1 inhibitor-dependent genomic damage and provide a rationale for the development of new approaches to sensitize cancer cells to chemotherapy.

Acknowledgements

This work is dedicated to the memory of Dr Maria Malanga who died in November 2011, her good spirit, her ideas, her friendship and her energy are greatly missed by all her colleagues. We acknowledge Dr. Daria Maria Monti and Dr. Angela Arciello for their help with cell cultures.

References

- [1] Rouleau M, Patel A, Hendzel MJ, Kaufmann SH, Poirier GG. PARP inhibition: PARP1 and beyond. *Nat Rev Cancer* 2010;10:293–301.
- [2] Burkle A. Poly(ADP-ribosylation). *LANDES Biosci* 2005.
- [3] Malanga M, Althaus FR. The role of poly(ADP-ribose) in the DNA damage signaling network. *Biochem Cell Biol* 2005;83(3):354–64.
- [4] Schreiber V, Dantzer F, Ame JC, de Murcia G. Poly(ADP-ribose): novel function for an old molecule. *Nat Rev Mol Cell Biol* 2006;7:517–28.

- [5] Sugimura K, Takebayashi S, Taguchi H, Takeda S, Okumura K. PARP1 ensures regulation of replication fork progression by homologous recombination on damaged DNA. *J Cell Biol* 2008;183:1203–12.
- [6] Malanga M, Althaus FR. Poly(ADP-ribose) reactivates stalled DNA topoisomerase I and induces DNA strand break resealing. *J Biol Chem* 2004;279(7):5244–8.
- [7] Mitchell J, Smith GC, Curtin NJ. Poly(ADP-Ribose) polymerase-1 and DNA-dependent protein kinase have equivalent roles in double strand break repair following ionizing radiation. *Int J Radiat Oncol Biol Phys* 2009;75(5):1520–7.
- [8] Haince JF, Kozlov S, Dawson VL, Dawson TM, Hendzel MJ, Lavin MF, et al. Ataxia telangiectasia mutated (ATM) signaling network is modulated by a novel poly(ADP-ribose)-dependent pathway in the early response to DNA-damaging agents. *J Biol Chem* 2007;282:16441–53.
- [9] Yoon JH, Ahn SG, Lee BH, Jung SH, Oh SH. Role of autophagy in chemoresistance: regulation of the ATM-mediated DNA-damage signaling pathway through activation of DNA-PKcs and PARP1. *Biochem Pharmacol* 2012;83(6):747–57.
- [10] Nguyen D, Zajac-Kaye M, Rubinstein L, Voeller D, Tomaszewski JE, Kummar S, et al. Poly(ADP-ribose) polymerase inhibition enhances p53-dependent and -independent DNA damage responses induced by DNA damaging agent. *Cell Cycle* 2011;10(23):4074–82.
- [11] Wieler S, Gagne' JP, Vaziri H, Poirier GG, Benchimol S. Poly(ADP-ribose) Polymerase-1 is a positive regulator of the p53-mediated G1 arrest response following ionizing radiation. *J Biol Chem* 2003;278:18914–21.
- [12] Cazzalini O, Donà F, Savio M, Tillhon M, Maccario C, Perucca P, et al. p21CDKN1A participates in base excision repair by regulating the activity of poly(ADP-ribose) polymerase. *DNA Repair* 2010;9(6):627–35.
- [13] Tentori L, Graziani G. Chemopotentiation by PARP inhibitors in cancer therapy. *Pharmacol Res* 2005;52:25–33.
- [14] Sandhu SK, Yap TA, de Bono JS. Poly(ADP-ribose) polymerase inhibitors in cancer treatment: a clinical perspective. *Eur J Cancer* 2010;46(1):9–20.
- [15] Smith LM, Willmore E, Austin CA, Curtin NJ. The novel poly(ADP-Ribose) polymerase inhibitor, AG14361, sensitizes cells to topoisomerase I poisons by increasing the persistence of DNA strand breaks. *Clin Cancer Res* 2005;11:8449–57.
- [16] Pommier Y. Topoisomerase I inhibitors: camptothecins and beyond. *Nat Rev Cancer* 2006;6:789–802.
- [17] Arnaudeau C, Lundin C, Helleday T. DNA double-strand breaks associated with replication forks are predominantly repaired by homologous recombination involving an exchange mechanism in mammalian cells. *J Mol Biol* 2001;307:1235–45.
- [18] Cimmino G, Pepe S, Laus G, Chianese M, Prece D, Penitente R, et al. Poly(-ADPR)polymerase-1 signaling of the DNA damage induced by DNA topoisomerase I poison in D54(p53 wt) and U251(p53mut) glioblastoma cell lines. *Pharmacol Res* 2007;55(1):49–56.
- [19] Gambi N, Tramontano F, Quesada P. Poly(ADPR)polymerase inhibition and apoptosis induction in cDDP-treated human carcinoma cell lines. *Biochem Pharmacol* 2008;75(12):2356–63.
- [20] D'Onofrio G, Tramontano F, Dorio AS, Muzi A, Maselli V, Fulgione D, et al. Poly(ADP-Ribose) Polymerase signaling of topoisomerase 1-dependent DNA damage in carcinoma cells. *Biochem Pharmacol* 2011;81:194–202.
- [21] Madison DL, Stauffer D, Lundblad JR. The PARP inhibitor PJ34 causes a PARP1-independent, p21 dependent mitotic arrest. *DNA Repair (Amst)* 2011;10(10):1003–13.
- [22] Hastak K, Alli E, Ford JM. Synergistic chemosensitivity of triple-negative breast cancer cell lines to PARP inhibition, gemcitabine and cisplatin. *Cancer Res* 2010;70(20):7970–80.
- [23] Di Costanzo A, Troiano A, di Martino O, Cacace A, Natale CF, Ventre M, et al. The p63 Protein Isoform {Delta}Np63 α Modulates Y-box Binding Protein 1 in Its Subcellular Distribution and Regulation of Cell Survival and Motility Genes. *J Biol Chem* 2012;287(36):30170–80.
- [24] Di Costanzo A, Festa L, Roscigno G, Vivo M, Pollice A, Morasso M, et al. A dominant mutation etiologic for human Tricho-Dento-Osseus syndrome impairs the ability of DLX3 to downregulate Δ Np63 α . *J Cell Physiol* 2011;226(8):2189–97.
- [25] Schavolt KL, Pietenpol JA. p53 and Delta Np63 alpha differentially bind and regulate target genes involved in cell cycle arrest, DNA repair and apoptosis. *Oncogene* 2007;26:6125–32.
- [26] Yang A, Kaghad M, Wang Y, Gillett E, Fleming MD, Dötsch V, et al. p63, a p53 homolog at 3q27–29, encodes multiple products with transactivating, death-inducing, and dominant-negative activities. *Mol Cell* 1998;2(3):305–16.
- [27] Devy J, Wargnier R, Pluot M, Nabiev I, Sukhanova A. Topotecan-induced alterations in the amount and stability of human DNA topoisomerase I in solid tumor cell lines. *Anticancer Res* 2004;24(3a):1745–51.
- [28] Rocco JW, Leong CO, Kuperwasser N, DeYoung MP, Ellisen LW. p63 mediates survival in squamous cell carcinoma by suppression of p73-dependent apoptosis. *Cancer Cell* 2006;9(1):45–56.
- [29] Bryant HE, Schultz N, Thomas HD, Parker KM, Flower D, Lopez E, et al. Specific killing of BRCA2-deficient tumours with inhibitors of poly(ADP-ribose) polymerase. *Nature* 2005;434(7035):913.
- [30] Feeney GP, Errington RJ, Wiltshire M, Marquez N, Chappell SC, Smith PJ. Tracking the cell cycle origins for escape from topotecan action by breast cancer cells. *Br J Cancer* 2003;88(8):1310–7.
- [31] Davis PL, Shaiu WL, Scott GL, Iglehart JD, Hsieh TS, Marks JR. Complex response of breast epithelial cell lines to topoisomerase inhibitors. *Anticancer Res J* 1998;18(4C):2919–32.
- [32] Yang A, Kaghad M, Wang Y, Gillett E, Fleming MD, Dötsch V, et al. p63, a p53 homolog at 3q27–29 encodes multiple products with transactivating death-inducing and dominant-negative activities. *Mol Cell* 1998;2(3):305–16.
- [33] Sugimura K, Takebayashi S, Taguchi H, Takeda S, Okumura K. PARP-1 ensures regulation of replication fork progression by homologous recombination on damaged DNA. *J Cell Biol* 2008;183:1203–12.
- [34] Chaudhuri AR, Hashimoto Y, Herradori R, Neelsen KJ, Fachinetti D, Bermejo R, et al. Topoisomerase I poisoning results in PARP-mediated replication fork reversal. *Nat Struct Mol Biol* 2012;19(4):417–24.
- [35] Malanga M, Pleschke JM, Kleczkowska HE, Althaus FR. Poly(ADP-ribose) binds to specific domains of p53 and alters its DNA binding functions. *J Biol Chem* 2000;275:40974–80.
- [36] Kanai M, Hanashiro K, Kim So H, Hanai S, Boulares HA, Miwa M, et al. Inhibition of Crm1–p53 interaction and nuclear export of p53 by poly(ADP-ribosylation). *Nat Cell Biol* 2007;9(10):1175–83.